

Pre-Born–Oppenheimer Molecular Structure Theory

Edit Mátyus, ELTE Budapest

(Dated: 31 August, 2017)

These lecture notes are intended for an introduction to pre-Born–Oppenheimer (pre-BO) theory. Alternatively, they can also be considered as a short course on variational techniques for the example of computing molecules without the BO approximation.

Recommended literature:

- Y. Suzuki and K. Varga, **Stochastic Variational Approach to Quantum-Mechanical Few-Body Problems**, Springer-Verlag (Berlin, 1998)

I. THE MANY-PARTICLE SCHRÖDINGER EQUATION

$$\hat{H}\Psi = E\Psi \quad (1)$$

with

$$\hat{H}(\mathbf{m}, \mathbf{q}; \mathbf{r}) = - \sum_{i=1}^{n_p+1} \frac{1}{2m_i} \Delta_{\mathbf{r}_i} + \sum_{i=1}^{n_p+1} \sum_{j>i}^{n_p+1} \frac{q_i q_j}{|\mathbf{r}_i - \mathbf{r}_j|} \quad (2)$$

where the mass and electric charge, m_i and q_i ($i = 1, 2, \dots, n_p + 1$), are constant parameters. In addition, physically meaningful solutions satisfy the spin-statistics theorem for fermions and bosons (“Pauli principle”), so we have to consider the spin (fermionic or bosonic character), s_i ($i = 1, 2, \dots, n_p + 1$), for each particle as an additional parameter.

There are in total $3(n_p + 1)$ physical parameters, $\{m_i, q_i, s_i (i = 1, 2, \dots, n_p + 1)\}$, which specify an isolated molecule.

The Hamiltonian is invariant to space rotations and inversion, furthermore it is independent of the particles’ spin. Thereby, the total angular momentum, \hat{N}^2 , its projection, \hat{N}_z , space inversion, \hat{i} , and the total spin angular momentum and its projection for each particle type, *e.g.*, a , \hat{S}_a^2 and $\hat{S}_{a,z}$ are conserved quantities, *i.e.*,

$$\left[\hat{H}, \hat{N}^2 \right] = 0 \quad \left[\hat{H}, \hat{N}_z \right] = 0 \quad (3)$$

$$\left[\hat{H}, \hat{i} \right] = 0 \quad (4)$$

$$\left[\hat{H}, \hat{S}_a^2 \right] = 0 \quad \left[\hat{H}, \hat{S}_{a,z} \right] = 0. \quad (5)$$

where the total angular momentum vector is the vector sum of the angular momentum of the particles

$$\hat{\mathbf{N}} = \sum_{i=1}^{n_p+1} \mathbf{r}_i \times \mathbf{p}_i. \quad (6)$$

II. VARIATIONAL PRINCIPLES

Ritz theorem: For an arbitrary φ function in the state space the Rayleigh quotient is an upper bound to the ground-state energy.

The Hamiltonian, \hat{H} , is Hermitian operator, bounded from below and time independent.

$$\hat{H}\Psi_i = E_i\Psi_i \quad (7)$$

where the eigenvalues are ordered as: $E_1 < E_2 \leq E_3 \leq \dots$. For some (normalizable) φ the Rayleigh quotient is

$$\varepsilon = \frac{\langle \varphi | \hat{H} | \varphi \rangle}{\langle \varphi | \varphi \rangle}. \quad (8)$$

The theorem states that

$$\varepsilon \geq E_1. \quad (9)$$

Proof: Let us expand φ in terms of the Ψ_i eigenstates of \hat{H} :

$$\varphi = \sum_{i=1} c_i \Psi_i. \quad (10)$$

Then,

$$\begin{aligned} \varepsilon - E_1 &= \frac{\langle \varphi | \hat{H} | \varphi \rangle}{\langle \varphi | \varphi \rangle} - E_1 \\ &= \frac{\sum_{i=1} \sum_{j=1} c_i^* c_j \langle \Psi_i | \hat{H} | \Psi_j \rangle}{\sum_{i=1} \sum_{j=1} c_i^* c_j \langle \Psi_i | \Psi_j \rangle} - E_1 \\ &= \frac{\sum_{i=1} \sum_{j=1} c_i^* c_j E_j \delta_{ij}}{c_i^* c_j \delta_{ij}} - E_1 \\ &= \frac{\sum_{i=1} |c_i|^2 (E_j - E_1)}{\sum_{i=1} |c_i|^2} \geq 0. \end{aligned} \quad (11)$$

Generalized Ritz theorem: *The expectation value of \hat{H} is stationary in the neighborhood of its discrete eigenvalues.*

$$\delta E = 0 \quad \text{upon any } \delta\Psi \quad \text{for } \hat{H}\Psi = E\Psi \quad (12)$$

Proof: The energy functional is

$$E = \frac{\langle\Psi|\hat{H}|\Psi\rangle}{\langle\Psi|\Psi\rangle}. \quad (13)$$

The variation of the energy functional upon a small, $\delta\Psi$ variation of the wave function is:

$$\begin{aligned} \delta E &= \frac{\langle\delta\Psi|\hat{H}|\Psi\rangle\langle\Psi|\Psi\rangle - \langle\delta\Psi|\Psi\rangle\langle\Psi|\hat{H}|\Psi\rangle}{\langle\Psi|\Psi\rangle^2} + \text{cc.} \\ &= \frac{E\langle\delta\Psi|\Psi\rangle\langle\Psi|\Psi\rangle - \langle\delta\Psi|\Psi\rangle E\langle\Psi|\Psi\rangle}{\langle\Psi|\Psi\rangle^2} + \text{cc.} \\ &= 0. \end{aligned} \quad (14)$$

Linear variational method: *Due to the generalized Ritz principle, the computation of eigenvalues and eigenvectors in a finite basis set is translated to a matrix-eigenvalue problem.* Let us consider a \mathcal{V}_K subspace spanned by the $\psi_1, \psi_2, \dots, \psi_K$ functions. Then, we approximate the exact wave function on this subspace as a linear combination

$$\Psi_{\mathcal{V}} = \sum_{i=1}^K c_i \psi_i. \quad (15)$$

Substituting this form into the generalized variational principle:

$$\begin{aligned}
0 &= \langle \delta\Psi | (\hat{H} - E) \Psi \rangle \\
&= \langle \delta \sum_{i=1}^K c_i \psi_i | (\hat{H} - E) \sum_{j=1}^K c_j \psi_j \rangle \\
&= \sum_{i=1}^K \sum_{j=1}^K \delta c_i^* c_j \langle \psi_i | (\hat{H} - E) | \psi_j \rangle \\
&= \sum_{i=1}^K \delta c_i^* \sum_{j=1}^K (H_{ij} - ES_{ij}) c_j.
\end{aligned} \tag{16}$$

So, for any small δc_i variation we require:

$$\sum_{j=1}^K (H_{ij} - ES_{ij}) c_j = 0, \quad \text{for all } i = 1, \dots, K, \tag{17}$$

which is equivalent to the matrix eigenvalue problem

$$\mathbf{H}\mathbf{c} = E\mathbf{S}\mathbf{c}. \tag{18}$$

The matrix elements of the Hamiltonian are

$$H_{ij} = \langle \psi_i | \hat{H} | \psi_j \rangle \tag{19}$$

and the overlap matrix elements are

$$S_{ij} = \langle \psi_i | \psi_j \rangle, \tag{20}$$

which is the $K \times K$ unit matrix if $\psi_1, \psi_2, \dots, \psi_K$ are orthonormal functions.

Theorem *about enlargement of the basis set and the variational property of excited states:* “Upon enlargement of the basis set, the eigenvalues never get worse.” (\Rightarrow Figure)

Let $\varepsilon_1 \leq \varepsilon_2 \leq \dots \leq \varepsilon_K$ be the eigenvalues of \hat{H} on a subspace \mathcal{V}_K spanned by the $\psi_1, \psi_2, \dots, \psi_K$ independent functions.

Let $\varepsilon'_1 \leq \varepsilon'_2 \leq \dots \leq \varepsilon'_K + 1$ be the eigenvalues of \hat{H} on a subspace \mathcal{V}_{K+1} spanned by the independent functions $\psi_1, \psi_2, \dots, \psi_K, \psi_{K+1}$.

Then:

$$\varepsilon'_1 \leq \varepsilon_1 \leq \varepsilon'_2 \leq \varepsilon_2 \leq \dots \varepsilon'_K \leq \varepsilon_K \leq \varepsilon_{K+1}. \quad (21)$$

Proof: Let $\phi_1, \phi_2, \dots, \phi_K$ be the orthonormal eigenstates corresponding to the eigenvalues $\varepsilon_1, \varepsilon_2, \dots, \varepsilon_K$. Then, any function Ψ in \mathcal{V}_{K+1} can be expressed as

$$\Psi = \sum_{i=1}^{K+1} c_i \phi_i \quad (22)$$

where the $(K + 1)$ th orthonormal function is obtained as follows.

$$\begin{aligned} |\phi_{K+1}\rangle &= \frac{1}{\sqrt{N}} \left[|\psi_{K+1}\rangle - \sum_{i=1}^K |\phi_i\rangle \frac{\langle \phi_i | \psi_{K+1} \rangle}{\langle \phi_i | \phi_i \rangle} \right] \\ &= \frac{1}{\sqrt{N}} \left[|\psi_{K+1}\rangle - \sum_{i=1}^K |\phi_i\rangle \langle \phi_i | \psi_{K+1} \rangle \right], \end{aligned} \quad (23)$$

where the N normalization constant is

$$\begin{aligned} N &= \left\langle \psi_{K+1} - \sum_{i=1}^K \langle \phi_i | \psi_{K+1} \rangle \phi_i \middle| \psi_{K+1} - \sum_{j=1}^K \langle \phi_j | \psi_{K+1} \rangle \phi_j \right\rangle \\ &= \langle \psi_{K+1} | \psi_{K+1} \rangle - 2 \sum_{i=1}^K \langle \phi_i | \psi_{K+1} \rangle^* \langle \phi_i | \psi_{K+1} \rangle + \sum_{i=1}^K \sum_{j=1}^K \langle \phi_i | \psi_{K+1} \rangle^* \langle \phi_j | \psi_{K+1} \rangle \langle \phi_i | \phi_j \rangle \\ &= \langle \psi_{K+1} | \psi_{K+1} \rangle - \sum_{i=1}^K |\langle \phi_i | \psi_{K+1} \rangle|^2. \end{aligned} \quad (24)$$

The eigenvalue problem using the basis set $\phi_1, \phi_2, \dots, \phi_K, \phi_{K+1}$ is:

$$\begin{pmatrix} \varepsilon_1 & 0 & \dots & 0 & h_1 \\ 0 & \varepsilon_2 & \dots & 0 & h_2 \\ \vdots & \vdots & \ddots & \vdots & \vdots \\ 0 & 0 & \dots & \varepsilon_K & h_K \\ h_1^* & h_2^* & \dots & h_K^* & h_{K+1} \end{pmatrix} \begin{pmatrix} c_1 \\ c_2 \\ \vdots \\ c_K \\ c_{K+1} \end{pmatrix} = E \begin{pmatrix} c_1 \\ c_2 \\ \vdots \\ c_K \\ c_{K+1} \end{pmatrix} \quad (25)$$

where

$$h_j = \langle \phi_j | \hat{H} \phi_{K+1} \rangle. \quad (26)$$

In order to solve this eigenvalue problem, we rearrange the equation to

$$\begin{pmatrix} \varepsilon_1 - E & 0 & \dots & 0 & h_1 \\ 0 & \varepsilon_2 - E & \dots & 0 & h_2 \\ \vdots & \vdots & \ddots & \vdots & \vdots \\ 0 & 0 & \dots & \varepsilon_K - E & h_K \\ h_1^* & h_2^* & \dots & h_K^* & h_{K+1} - E \end{pmatrix} \begin{pmatrix} c_1 \\ c_2 \\ \vdots \\ c_K \\ c_{K+1} \end{pmatrix} = 0. \quad (27)$$

The new eigenvalues are obtained as the roots of the $D(E)$ characteristic function, the determinant of the matrix in the left hand side of Eq. (27). We expand the determinant by its last column, and then, the corresponding minor is expanded (trivially) by its last row: (\Rightarrow Figure)

$$\begin{aligned} 0 &= D(E) \\ &= \det \begin{pmatrix} \varepsilon_1 - E & 0 & \dots & 0 & h_1 \\ 0 & \varepsilon_2 - E & \dots & 0 & h_2 \\ \vdots & \vdots & \ddots & \vdots & \vdots \\ 0 & 0 & \dots & \varepsilon_K - E & h_K \\ h_1^* & h_2^* & \dots & h_K^* & h_{K+1} - E \end{pmatrix} \\ &= (h_{K+1} - E) \prod_{j=1}^K (\varepsilon_j - E) + \sum_{i=1}^K h_i (-1)^{i+K+1} \det(\mathcal{A}_{i,K+1}) \\ &= (h_{K+1} - E) \prod_{j=1}^K (\varepsilon_j - E) + \sum_{i=1}^K h_i (-1)^{i+K+1} \left(h_i^* (-1)^{i+K} \frac{\prod_{j=1}^K (\varepsilon_j - E)}{\varepsilon_i - E} \right) \\ &= \prod_{j=1}^K (\varepsilon_j - E) \left[h_{K+1} - E - \sum_{i=1}^K \frac{|h_i|^2}{\varepsilon_i - E} \right] \end{aligned} \quad (28)$$

The new $(K + 1)$ eigenvalues are obtained by finding the roots of the equation

$$0 = \prod_{j=1}^K (\varepsilon_j - E) \left[h_{K+1} - E - \sum_{i=1}^K \frac{|h_i|^2}{\varepsilon_i - E} \right]. \quad (29)$$

Note that we assumed that all $h_i \neq 0$. Thereby, for $E = \varepsilon_j$ the last term in the second parentheses tends to infinity. Since $E \neq \varepsilon_j$, a rearranged form of Eq. (29) results in the practical working equation (\Rightarrow Figure)

$$E - h_{K+1} = \sum_{i=1}^K \frac{|h_i|^2}{E - \varepsilon_i}. \quad (30)$$

The theorem implies the variational property for not only the lowest but also for excited states. Furthermore, it offers a practical and efficient technique to compute the new eigenvalues upon the enlargement (or update) of the basis set if the “old” eigenvalues and eigenvectors are known.

A variational recipe In order to define a variational approach, it is necessary to specify the following details:

- coordinates
- Hamiltonian in the selected coordinates
- basis functions
- (analytic) matrix elements
- eigensolver
- optional: parameterization of the basis functions

III. COORDINATES

The full many-particle Hamiltonian has a continuous spectrum due to the overall translation of the system. Since we are interested in the “internal”, *translationally invariant* properties, we shall introduce translationally invariant Cartesian coordinates (TICCs).

The laboratory-fixed Cartesian coordinates (LFCCs) of a particle are labelled with $\mathbf{r}_i \in \mathbb{R}^3$ ($i = 1, 2, \dots, n_p + 1$). We define new Cartesian coordinates as a linear combination of \mathbf{r}_i with the following properties:

1. TI property: invariance upon a uniform translation, $\mathbf{d} \in \mathbb{R}^3$, of the overall system:

$$\mathbf{x}_i(\{\mathbf{r}_i + \mathbf{d}\}) = \mathbf{x}_i(\{\mathbf{r}_i\}) \in \mathbb{R}^3, \quad i = 1, 2, \dots, n_p; \quad (31)$$

2. Overall translational motion:

$$\mathbf{X}(\{\mathbf{r}_i + \mathbf{d}\}) = \mathbf{x}(\{\mathbf{r}_i\}) + \mathbf{d} \in \mathbb{R}^3, \quad (32)$$

where we used the shorthand notation: $\{\mathbf{r}_i\} = \{\mathbf{r}_i, i = 1, 2, \dots, n_p + 1\}$.

A linear transformation of LFCCs

$$\begin{pmatrix} \mathbf{x} \\ \mathbf{X} \end{pmatrix} = (\mathbf{U} \otimes \mathbf{I}_3) \mathbf{r}, \quad (33)$$

which satisfies the (1)–(2) conditions can be formulated in terms of conditions for the elements of the $\mathbf{U} \in \mathbb{R}^{(n_p+1) \times (n_p+1)}$ matrix:

1. TI condition:

For all $i = 1, \dots, n_p$:

$$\mathbf{x}_i = \sum_{j=1}^{n_p+1} U_{ij} \mathbf{r}_j \quad (34)$$

$$\begin{aligned} \mathbf{x}'_i &= \sum_{j=1}^{n_p+1} U_{ij} (\mathbf{r}_j + \mathbf{d}) \\ &= \sum_{j=1}^{n_p+1} U_{ij} \mathbf{r}_j + \sum_{j=1}^{n_p+1} U_{ij} \mathbf{d}. \end{aligned} \quad (35)$$

Due to the TI condition $\mathbf{x}_i = \mathbf{x}'_i$, and thus the last term in the last equation must vanish, which is fulfilled for any $\mathbf{d} \in \mathbb{R}^3$ if

$$\sum_{j=1}^{n_p+1} U_{ij} = 0, \quad i = 1, 2, \dots, n_p. \quad (36)$$

2. Translational condition:

$$\mathbf{X} = \sum_{j=1}^{n_p+1} U_{n_p+1,j} \mathbf{r}_j \quad (37)$$

$$\begin{aligned} \mathbf{X}' &= \sum_{j=1}^{n_p+1} U_{n_p+1,j} (\mathbf{r}_j + \mathbf{d}) \\ &= \sum_{j=1}^{n_p+1} U_{n_p+1,j} \mathbf{r}_j + \sum_{j=1}^{n_p+1} U_{n_p+1,j} \mathbf{d}. \end{aligned} \quad (38)$$

Due to the translational condition $\mathbf{X}' = \mathbf{X} + \mathbf{d}$, and thus the last term in the last equation must equal to \mathbf{d} , which is fulfilled if

$$\sum_{j=1}^{n_p+1} U_{n_p+1,j} = 1. \quad (39)$$

Any \mathbf{U} matrix which satisfies Eqs. (36) and (39) will define a TICC set and can be used to describe the internal motion.

Note that a convenient choice (see also the next section) to satisfy the translational condition, Eq. (39), is

$$U_{n_p+1,j} = \frac{m_j}{m_{\text{tot}}} \quad (40)$$

with

$$m_{\text{tot}} = \sum_{i=1}^{n_p+1} m_i \quad (41)$$

and m_i being the physical masses of the particles. For the following sections, we shall adopt this choice, and thus \mathbf{X} collects the center-of-mass Cartesian coordinates (CMCCs):

$$\mathbf{X}_{\text{CM}} = \sum_{i=1}^{n_p} \frac{m_i}{m_{\text{tot}}} \mathbf{r}_i. \quad (42)$$

For a short notation, we introduce $\tilde{\mathbf{x}}$:

$$\tilde{\mathbf{x}} = \begin{pmatrix} \mathbf{x} \\ \mathbf{X}_{\text{CM}} \end{pmatrix}. \quad (43)$$

Also note that \mathbf{U} is constant, hence the new coordinates are rectilinear.

There are various common choices for TICCs, for example (see also Figure 1)

- Jacobi coordinates (orthogonal)
- heavy-particle-centered coordinates
- center-of-mass-centered coordinates
- ...

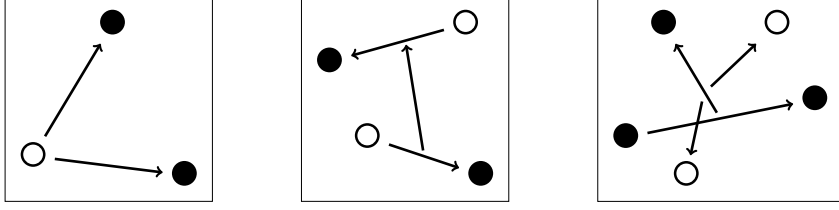


FIG. 1: Example for translationally invariant coordinate definitions.

A. Transformation of coordinates upon the permutation of identical particles

The permutation, \hat{P} of identical particles can be represented by a linear transformation of the LF Cartesian coordinates as

$$\mathbf{r}_P = \hat{P}\mathbf{r} = (\mathbf{T}_P \otimes \mathbf{I}_3)\mathbf{r}. \quad (44)$$

Since identical particles have the same mass, the CMCCs are unaffected, however the TICCs may change:

$$\begin{aligned} \tilde{\mathbf{x}}_P &= (\mathbf{U} \otimes \mathbf{I}_3)\mathbf{r}_P \\ &= (\mathbf{U} \otimes \mathbf{I}_3)(\mathbf{T}_P \otimes \mathbf{I}_3)\mathbf{r} \\ &= (\mathbf{U}\mathbf{T}_P \otimes \mathbf{I}_3)\mathbf{r} \end{aligned} \quad (45)$$

It can be shown that $\mathbf{U}\mathbf{T}_P$ also satisfies the TI and translational conditions, and thus the permutation of identical particles does not affect translational invariance, but it may result in another set of TICCs. (\Rightarrow Figure)

IV. QUANTUM HAMILTONIANS

$$\hat{H} = \hat{T}' + \hat{V}(|\mathbf{r}_i - \mathbf{r}_j|) \quad (46)$$

The Coulomb potential energy depends on the distance between pairs of particles, so it is translationally invariant. In this section, we focus on the separation of the overall translation from the kinetic energy operator (KEO) and express the KEO in terms of translationally invariant coordinates and center-of-mass Cartesian coordinates, introduced in the previous section.

The $(n_p + 1)$ -particle kinetic-energy operator is

$$\hat{T}' = - \sum_{i=1}^{n_p+1} \frac{1}{2m_i} \Delta_{\mathbf{r}_i} = - \sum_{i=1}^{n_p+1} \frac{1}{2m_i} \left(\frac{\partial^2}{\partial r_{ix}^2} + \frac{\partial^2}{\partial r_{iy}^2} + \frac{\partial^2}{\partial r_{iz}^2} \right), \quad (47)$$

which will be written in terms of the new coordinates by using the chain rule:

$$\tilde{\mathbf{x}} = \begin{pmatrix} \mathbf{x} \\ \mathbf{X}_{\text{CM}} \end{pmatrix} = (\mathbf{U} \otimes \mathbf{I}_3) \mathbf{r}, \quad (48)$$

which is for the elements ($\alpha = x, y, z$):

$$\tilde{x}_{j\alpha} = \sum_{j=1}^{n_p+1} U_{ji} r_{i\alpha}. \quad (49)$$

Then, we write down the first derivative in terms of $\tilde{x}_{j\alpha}$ as

$$\frac{\partial}{\partial r_{i\alpha}} = \sum_{j=1}^{n_p+1} \frac{\partial \tilde{x}_{j\alpha}}{\partial r_{i\alpha}} \frac{\partial}{\partial \tilde{x}_{j\alpha}} = \sum_{j=1}^{n_p+1} U_{ji} \frac{\partial}{\partial \tilde{x}_{j\alpha}} \quad (50)$$

The second derivative is rearranged as follows:

$$\begin{aligned}
& \sum_{i=1}^{n_p+1} \frac{1}{m_i} \frac{\partial^2}{\partial r_{i\alpha}^2} \\
&= \sum_{i=1}^{n_p+1} \frac{1}{m_i} \left[\sum_{j=1}^{n_p+1} U_{ji} \frac{\partial}{\partial \tilde{x}_{j\alpha}} \left(\sum_{k=1}^{n_p+1} U_{ki} \frac{\partial}{\partial \tilde{x}_{k\alpha}} \right) \right] \\
&= \sum_{i=1}^{n_p+1} \frac{1}{m_i} \left[\left(\sum_{j=1}^{n_p+1} \sum_{k=1}^{n_p+1} U_{ji} U_{ki} \right) \frac{\partial}{\partial \tilde{x}_{j\alpha}} \frac{\partial}{\partial \tilde{x}_{k\alpha}} \right] \\
&= \sum_{i=1}^{n_p+1} \frac{1}{m_i} \left[\left(\sum_{j=1}^{n_p} \sum_{k=1}^{n_p} U_{ji} U_{ki} \frac{\partial^2}{\partial x_{j\alpha} \partial x_{k\alpha}} + 2 \sum_{j=1}^{n_p+1} U_{ji} U_{n_p+1,i} \frac{\partial}{\partial x_{j\alpha}} \frac{\partial}{\partial X_\alpha} + U_{n_p+1,i}^2 \frac{\partial^2}{\partial X_\alpha^2} \right) \right] \\
&= \sum_{j=1}^{n_p} \sum_{k=1}^{n_p} \sum_{i=1}^{n_p+1} \frac{1}{m_i} U_{ji} U_{ki} \frac{\partial^2}{\partial x_{j\alpha} \partial x_{k\alpha}} \\
&\quad + 2 \sum_{j=1}^{n_p+1} \sum_{i=1}^{n_p+1} \frac{1}{m_i} U_{ji} \frac{m_i}{m_{\text{tot}}} \frac{\partial}{\partial x_{j\alpha}} \frac{\partial}{\partial X_\alpha} \\
&\quad + \sum_{i=1}^{n_p+1} \frac{1}{m_i} \left(\frac{m_i}{m_{\text{tot}}} \right)^2 \frac{\partial^2}{\partial X_\alpha^2}, \tag{51}
\end{aligned}$$

where in the last equation the second term—which corresponds to the coupling of the TI and center-of-mass coordinates—is zero due to the TI condition:

$$\sum_{i=1}^{n_p+1} \frac{1}{m_i} U_{ji} \frac{m_i}{m_{\text{tot}}} = 0, \tag{52}$$

and the last term corresponds to the α 's component of the kinetic energy of the center of mass:

$$\sum_{i=1}^{n_p+1} \frac{1}{m_i} \left(\frac{m_i}{m_{\text{tot}}} \right)^2 = \frac{1}{m_{\text{tot}}}. \tag{53}$$

Thereby, we can introduce the translationally invariant kinetic energy operator (remember that the TI and CM coupling terms vanish):

$$\begin{aligned}
\hat{T} &= \hat{T}' - \hat{T}_{\text{CM}} \\
&= \hat{T}' - \frac{1}{2m_{\text{tot}}} \Delta_{\mathbf{x}_{\text{CM}}} \\
&= -\frac{1}{2} \sum_{\alpha} \sum_{j=1}^{n_p} \sum_{k=1}^{n_p} \Lambda_{jk} \frac{\partial^2}{\partial x_{j\alpha} \partial x_{k\alpha}} \\
&= -\frac{1}{2} \sum_{j=1}^{n_p} \sum_{k=1}^{n_p} \Lambda_{jk} \nabla_{\mathbf{x}_j}^T \nabla_{\mathbf{x}_k}
\end{aligned} \tag{54}$$

with

$$\Lambda_{jk} = \sum_{i=1}^{n_p+1} \frac{1}{m_i} U_{ji} U_{ki}. \tag{55}$$

For a particular choice of the TI Cartesian coordinates the elements of the mass-scaled metric tensor, $\mathbf{\Lambda}$, can be calculated. For example, Jacobi coordinates are orthogonal, and thus $\mathbf{\Lambda}$ is diagonal: $\Lambda_{ij} = \delta_{ij} \frac{1}{\mu_i}$ with the μ_i Jacobi reduced mass.

V. BASIS FUNCTIONS

Ideally the basis functions span a space which include the exact eigenfunctions of the Hamiltonian. In practice, the space is enlarged so that the best eigenfunction approaches the exact solution. It is often preferred to define basis functions, which are eigenfunctions of the conserved quantities (“variation after projection”), but it is also possible to use basis functions which are not symmetry adapted and the symmetry is restored numerically during the course of the variational computation.

In what follows, we shall apply basis functions which are symmetry-adapted functions:

$$\Phi^{[\lambda, \varsigma]} = \hat{\mathcal{A}}\{\phi^{[\lambda]}\chi^{[\varsigma]}\}, \quad (56)$$

which is an (anti)symmetrized product of spatial functions, $\phi^{[\lambda]}$, and spin functions, $\chi^{[\varsigma]}$. The spatial and spin functions are eigenfunctions of the total angular momentum and the parity, $\lambda = (N, M_N, p)$, and the spin angular momentum operators, $\varsigma = (S_a, M_{S_a}, S_b, M_{S_b}, \dots)$ (a, b, \dots denote the particle type), respectively. The symmetrization or antisymmetrization operator is

$$\hat{\mathcal{A}} = (N_{\text{perm}})^{-1/2} \sum_{p=1}^{N_{\text{perm}}} \varepsilon_p \hat{P}_p \quad (57)$$

for bosonic and fermionic-type particles. $\hat{P}_p \in \mathcal{S}_{n_a} \otimes \mathcal{S}_{n_b} \otimes \dots$ is an operator permuting identical particles and $\varepsilon_p = -1$ if \hat{P}_p represents an odd number of interchanges of fermions, otherwise $\varepsilon_p = +1$.

In a variational approach which uses symmetry-adapted basis functions, the quantum numbers corresponding to the conserved quantities can be specified on the “input” of a computation.

A. Spatial functions

We would like to use spatial functions which are

- square integrable
- positive definite
- analytic matrix elements for the common operators
- generally applicable for $(n_p + 1)$ -particle systems
- form (or approach to) a complete basis set

There are few candidates, which are known to have analytic matrix elements with the most common operators and are generally applicable to $(n_p + 1)$ -particle systems

1. Gaussian-type orbital: $\exp\left(-\frac{\alpha_i}{2}r_i^2\right)$
2. Gaussian-type geminal: $\exp\left(-\frac{\alpha}{2}(\mathbf{r}_i - \mathbf{r}_j)^2\right)$
3. many-particle explicitly correlated Gaussian (ECG): $\exp\left(-\frac{1}{2}\mathbf{r}^T(\mathbf{A} \otimes \mathbf{I}_3)\mathbf{r}\right)$
4. primitive ECG: $\exp\left(-\frac{1}{2}\mathbf{r}^T(\mathbf{A} \otimes \mathbf{I}_3)\mathbf{r} + \mathbf{s}^T\mathbf{r}\right)$
5. floating ECG: $\exp\left(-\frac{1}{2}(\mathbf{r} - \mathbf{R})^T(\mathbf{A} \otimes \mathbf{I}_3)(\mathbf{r} - \mathbf{R})\right)$
6. ECG with angular prefactor: $\theta(\mathbf{r}) \exp\left(-\frac{1}{2}\mathbf{r}^T(\mathbf{A} \otimes \mathbf{I}_3)\mathbf{r}\right)$

A few comments are in order:

- It is non-trivial but it can be shown that a Gaussian basis set is complete (“nodeless harmonic oscillator functions as a basis”...)
- Gaussian functions do not satisfy the cusp condition...
- Functions 1–3 are angular momentum and parity eigenfunctions with $N = 0$ and $p = +1$.
- Functions 4–5 are not angular momentum eigenfunctions unless $\mathbf{s} = 0$ and $\mathbf{R} = 0$, respectively, when they are $(N = 0, p = +1)$ functions.
- Function 6 can be made an angular momentum and parity eigenfunction ($N \geq 0$) with an appropriate choice of the angular prefactor.

1. *Angular symmetry, $\theta(\mathbf{r})$*

Solutions of the

$$\Delta_{\mathbf{r}} f(\mathbf{r}) = 0, \quad \mathbf{r} \in \mathbb{R}^3 \quad (58)$$

are the solid spherical harmonics ($l = 0, 1, \dots$ and $m = -l, \dots, l$)

$$f(\mathbf{r}) = r^l Y_{lm}(\hat{\mathbf{r}}) = \mathcal{Y}_{lm}(\mathbf{r}), \quad (59)$$

where

$$r = |\mathbf{r}| \quad \text{and} \quad \hat{\mathbf{r}} = \frac{1}{r} \mathbf{r} = \begin{pmatrix} \sin \vartheta \cos \varphi \\ \sin \vartheta \sin \varphi \\ \cos \vartheta \end{pmatrix} \quad (60)$$

and

$$Y_{lm}^*(\hat{\mathbf{r}}) = (-1)^l Y_{l,-m}(\hat{\mathbf{r}}). \quad (61)$$

Thereby, for the single-particle case and natural parity, $p = (-1)^L$, we may choose the angular prefactor as:

$$\theta_{LM}(\mathbf{r}) = \mathcal{Y}_{LM}(\mathbf{r}) = r^L Y_{LM}(\hat{\mathbf{r}}). \quad (62)$$

a. Vector-coupled product of solid spherical harmonics For the many-particle case with N particles, the angular prefactor can be defined as a vector-coupled product of solid spherical harmonics. (The total angular momentum is commonly denoted by L in the physics literature, while it is labeled with N in molecular spectroscopy. In this subsection, we shall use L for the total angular momentum and

N for the particle number to simplify notation.):

$$\begin{aligned}\theta_{LM}(\mathbf{r}) &= \left[[\mathcal{Y}_{l_1}(\mathbf{r}_1) \times \mathcal{Y}_{l_2}(\mathbf{r}_2)]_{L_{12}} \times \mathcal{Y}_{l_3}(\mathbf{r}_3) \right]_{L_{123}} \times \dots \times \mathcal{Y}_{l_N}(\mathbf{r}_N) \Big]_{LM} \\ &= \sum_{\kappa=\{m_1, m_2, \dots, m_N\}} c_\kappa \prod_{i=1}^N \mathcal{Y}_{l_i m_i}(\mathbf{r}_i)\end{aligned}\quad (63)$$

where c_κ is a product of Clebsch–Gordan coefficients needed to couple the orbital angular momenta to the specified quantum numbers, *e.g.*,

$$\begin{aligned}c_\kappa &= \langle l_1 m_1, l_2 m_2 | L_{12} m_1 + m_2 \rangle \langle L_{12} m_1 + m_2, l_3 m_3 | L_{123} m_1 + m_2 + m_3 \rangle \\ &\quad \cdot \dots \cdot \langle L_{12\dots N-1} m_1 + m_2 + \dots + m_{N-1}, l_N m_N | LM \rangle\end{aligned}\quad (64)$$

A few comments concerning this representation are collected in the following list:

- in this representation each relative motion has a definite angular momentum, *e.g.*, $L_{12}, \dots, L_{12\dots N-1}$;
- since the subsystems' angular momenta is not a conserved quantity, it may be important to include several sets of angular momenta $(l_1, l_2, \dots, l_N, L_{12}, L_{123}, \dots)$;
- when the inclusion of higher partial waves is necessary a faster convergence can be achieved with a particular set of angular momenta using different sets of relative coordinates;
- Since $\theta_{LM}(\mathbf{x})$ can be expressed by different partial-wave decompositions in different coordinate systems, we conclude that the partial-wave decomposition may not be so important after all.
- The evaluation of analytic matrix elements becomes intractable as the number of particles increases and higher and higher number of partial-wave contributions are included.
- These observations led to a different generalization of \mathcal{Y}_{LM} to the many-particle case.

b. Global vector representation Let us define a global vector (GV) as a linear combination of the particle coordinates

$$\mathbf{v} = \sum_{i=1}^N u_i \mathbf{r}_i = (\mathbf{u} \otimes \mathbf{I}_3)^T \mathbf{r} \quad (65)$$

and introduce the angular prefactor for this global vector as

$$\theta_{LM}(\mathbf{r}) = v^{2K+L} Y_{LM}(\hat{v}) = v^{2K} \mathcal{Y}_{LM}(\mathbf{v}). \quad (66)$$

Minimization of the energy functional with respect to \mathbf{u} will allow us to find the most suitable angle or linear combination of angles. The parameters u_1, u_2, \dots, u_N are continuous, which is an advantage in practice in comparison with the integer arrays of subsystems' angular momenta, $(l_1, l_2, \dots, l_N, L_{12}, L_{123}, \dots)$.

c. Relationship between the two forms of the many-particle angular factors

Theorem *about the equivalence of the global-vector representation (GVR) and a vector-coupled product representation in a variational procedure.*

Any GVR function

$$f(\mathbf{r}) = v^{2K} \mathcal{Y}_{LM}(\mathbf{v}) \quad \text{with} \quad \mathbf{v} = \sum_{i=1}^N u_i \mathbf{r}_i \quad (67)$$

can be expressed as a linear combination of vector-coupled products of solid spherical harmonics:

$$g(\mathbf{r}) = r_1^{2k_1} r_2^{2k_2} \dots r_N^{2k_N} \left[\left[[\mathcal{Y}_{l_1}(\mathbf{r}_1) \times \mathcal{Y}_{l_2}(\mathbf{r}_2)]_{L_{12}} \times \mathcal{Y}_{l_3}(\mathbf{r}_3) \right]_{L_{123}} \times \dots \times \mathcal{Y}_{l_N}(\mathbf{r}_N) \right]_{LM} \quad (68)$$

where $k_i, l_i \geq 0$ and $2k_1 + l_1 + 2k_2 + l_2 + \dots + 2k_N + l_N = 2K + L$.

Proof: Instead of presenting the full proof, which can be done by induction, we sketched the main steps for a two-particle case with $\mathbf{v} = \mathbf{r}_1 + \mathbf{r}_2$.

We shall express the integral

$$\mathcal{I} = \int d\hat{a} Y_{LM}(\hat{a})(\mathbf{a} \cdot \mathbf{v})^{2K+L} \quad (69)$$

both by GVR and by a linear combination of vector-coupled products. During the course of the calculations, we often use a known identity:

$$\begin{aligned} (\mathbf{a} \cdot \mathbf{r})^n &= \sum_{2k+l=n} B_{kl} a^{2k} r^{2k} \sum_{m=-l}^l \mathcal{Y}_{lm}^*(\mathbf{a}) \mathcal{Y}_{lm}(\mathbf{r}) \\ &= \sum_{2k+l=n} B_{kl} a^{2k} r^{2k} (-1)^l \sqrt{2l+1} [\mathcal{Y}_l(\mathbf{a}) \times \mathcal{Y}_l(\mathbf{r})]_{00} \end{aligned} \quad (70)$$

with

$$B_{kl} = \frac{4\pi(2k+l)!}{2^k k! (2k+2l+1)!!} \quad (71)$$

Using this identity, we write the integral as

$$\begin{aligned} \mathcal{I} &= \int d\hat{a} Y_{LM}(\hat{a}) \sum_{2k+l=2K+L} B_{kl} a^{2k} v^{2k} \sum_{m=-l}^l a^l Y_{lm}^*(\hat{a}) v^l Y_{lm}(\hat{v}) \\ &= \sum_{2k+l=2K+L} B_{kl} a^{2k} v^{2k} \sum_{m=-l}^l a^l v^l Y_{lm}(\hat{v}) \int d\hat{a} Y_{LM}(\hat{a}) Y_{lm}^*(\hat{a}) \\ &= \sum_{2k+l=2K+L} B_{kl} a^{2k} v^{2k} \sum_{m=-l}^l a^l v^l Y_{lm}(\hat{v}) \delta_{lL} \delta_{mM} \\ &= B_{kL} a^{2k+L} v^{2k+L} Y_{LM}(\hat{v}) \end{aligned} \quad (72)$$

An alternative way of writing \mathcal{I} starts with a direct expansion of the polynomial:

$$\begin{aligned}
& (\mathbf{a} \cdot \mathbf{r}_1 + \mathbf{a} \cdot \mathbf{r}_2)^{2K+L} \\
&= \sum_{p+q=2K+L} \frac{(2K+L)!}{p!q!} (\mathbf{a} \cdot \mathbf{r}_1)^p (\mathbf{a} \cdot \mathbf{r}_2)^q \\
&= \sum_{p+q=2K+L} \frac{(2K+L)!}{p!q!} \left[\sum_{2k_1+l_1=p} B_{k_1 l_1} a^{2k_1} r_1^{2k_1} (-1)^{l_1} \sqrt{2l_1+1} [\mathcal{Y}_{l_1}(\mathbf{a}) \times \mathcal{Y}_{l_1}(\mathbf{r}_1)]_{00} \right] \\
&\quad \left[\sum_{2k_2+l_2=q} B_{k_2 l_2} a^{2k_2} r_2^{2k_2} (-1)^{l_2} \sqrt{2l_2+1} [\mathcal{Y}_{l_2}(\mathbf{a}) \times \mathcal{Y}_{l_2}(\mathbf{r}_2)]_{00} \right].
\end{aligned} \tag{73}$$

It is possible to simplify the \hat{a} -dependent integral of the multiple spherical harmonics functions as

$$\begin{aligned}
& \int d\hat{a} Y_{LM}(\hat{a}) [\mathcal{Y}_{l_1}(\mathbf{a}) \times \mathcal{Y}_{l_1}(\mathbf{r}_1)]_{00} [\mathcal{Y}_{l_2}(\mathbf{a}) \times \mathcal{Y}_{l_2}(\mathbf{r}_2)]_{00} \\
&= \sum_{\lambda} \sqrt{\frac{2\lambda+1}{(2l_1+1)(2l_2+1)}} a^{l_1+l_2} C(l_1 l_2; \lambda) \\
&\quad \int d\hat{a} Y_{LM}(\hat{a}) [Y_{\lambda}(\hat{a}) \times [\mathcal{Y}_{l_1}(\mathbf{r}_1) \times \mathcal{Y}_{l_2}(\mathbf{r}_2)]_{\lambda}]_{00} \\
&= \sum_{\lambda} \sqrt{\frac{2\lambda+1}{(2l_1+1)(2l_2+1)}} a^{l_1+l_2} C(l_1 l_2; \lambda) \delta_{\lambda L} \frac{(-1)^L}{\sqrt{2L+1}} [\mathcal{Y}_{l_1}(\mathbf{r}_1) \times \mathcal{Y}_{l_2}(\mathbf{r}_2)]_{LM} \\
&= a^{l_1+l_2} \frac{(-1)^L C(l_1 l_2; L)}{\sqrt{(2l_1+1)(2l_2+1)}} [\mathcal{Y}_{l_1}(\mathbf{r}_1) \times \mathcal{Y}_{l_2}(\mathbf{r}_2)]_{LM}
\end{aligned} \tag{74}$$

where we used that a vector-coupled product of two spherical harmonics with the same angles and an even $l+l'+L$ value can be written as

$$[Y_l(\hat{r}) \times Y_{l'}(\hat{r})]_{LM} = C(l l'; L) Y_{LM}(\hat{r}) \tag{75}$$

with

$$C(l l'; L) = \sqrt{\frac{(2l+1)(2l'+1)}{4\pi(2L+1)}} \langle 10 l' 0 | L 0 \rangle. \tag{76}$$

By plugging Eqs. (73) and (74) into the original integral, Eq. (69), we obtain

$$\begin{aligned}
\mathcal{I} &= \int d\hat{a} Y_{LM}(\hat{a})(\mathbf{a} \cdot \mathbf{v})^{2K+L} \\
&= \int d\hat{a} Y_{LM}(\hat{a})(\mathbf{a} \cdot \mathbf{r}_1 + \mathbf{a} \cdot \mathbf{r}_2)^{2K+L} \\
&= \sum_{p+q=2K+L} \frac{(2K+L)!}{p!q!} \sum_{2k_1+l_1=p} \sum_{2k_2+l_2=q} B_{k_1l_1} B_{k_2l_2} (-1)^{l_1+l_2} a^{2k_1+2k_2} r_1^{2k_1} r_2^{2k_2} \\
&\quad \int d\hat{a} Y_{LM}(\hat{a}) [\mathcal{Y}_{l_1}(\mathbf{a}) \times \mathcal{Y}_{l_1}(\mathbf{r}_1)]_{00} [\mathcal{Y}_{l_2}(\mathbf{a}) \times \mathcal{Y}_{l_2}(\mathbf{r}_2)]_{00} \\
&= \sum_{p+q=2K+L} \frac{(2K+L)!}{p!q!} \sum_{2k_1+l_1=p} \sum_{2k_2+l_2=q} B_{k_1l_1} B_{k_2l_2} (-1)^{l_1+l_2} a^{2k_1+2k_2} r_1^{2k_1} r_2^{2k_2} \\
&\quad a^{l_1+l_2} \frac{(-1)^L C(l_1 l_2; L)}{\sqrt{(2l_1+1)(2l_2+1)}} [\mathcal{Y}_{l_1}(\mathbf{r}_1) \times \mathcal{Y}_{l_2}(\mathbf{r}_2)]_{LM} \\
&= \sum_{p+q=2K+L} \sum_{2k_1+l_1=p} \sum_{2k_2+l_2=q} \frac{(2K+L)!}{p!q!} B_{k_1l_1} B_{k_2l_2} \frac{(-1)^{L+l_1+l_2} C(l_1 l_2; L)}{\sqrt{(2l_1+1)(2l_2+1)}} \\
&\quad a^{2k_1+l_1+2k_2+l_2} x_1^{2k_1} + x_2^{2k_2} [\mathcal{Y}_{l_1}(\mathbf{r}_1) \times \mathcal{Y}_{l_2}(\mathbf{r}_2)]_{LM}. \tag{77}
\end{aligned}$$

We repeat the final expression of Eq. (72)

$$\mathcal{I} = B_{kL} a^{2k+L} v^{2k+L} Y_{LM}(\hat{v}), \tag{78}$$

which completes the proof for the two-particle case, *i.e.*, the GVR angular function can be expressed in terms of linear combination of vector-coupled product spherical harmonics functions.

d. Generator integral for GVR There are many interesting mathematical properties of the angular functions in the different representations. We present in this paragraph an important property, which is extensively used during the course of the analytic calculation of the integrals of physical operators with GVR-ECG functions.

Statement about the relation of $r^{2K+L} Y_{LM}(\hat{r})$ and $e^{\lambda \mathbf{a} \cdot \mathbf{r}}$:

$$\int d\hat{a} Y_{LM}(\hat{a}) \left(\frac{\partial^{2K+L}}{\partial \lambda^{2K+L}} e^{\lambda \mathbf{a} \cdot \mathbf{r}} \right)_{\lambda=0, a=1} = B_{KL} r^{2K+L} Y_{LM}(\hat{r}) \tag{79}$$

Proof:

$$\begin{aligned}
\left(\frac{\partial^n}{\partial \lambda^n} e^{\lambda \mathbf{a} \cdot \mathbf{r}}\right)_{\lambda=0} &= \left(\frac{\partial^n}{\partial \lambda^n} \sum_{m=0}^{\infty} \frac{1}{m!} \lambda^m (\mathbf{a} \cdot \mathbf{r})^m\right)_{\lambda=0} \\
&= (\mathbf{a} \cdot \mathbf{r})^n \\
&= \sum_{2k+l=n} B_{kl} a^{2k+l} r^{2k+l} \sum_{m=-l}^l Y_{lm}^*(\hat{\mathbf{a}}) Y_{lm}(\hat{\mathbf{r}})
\end{aligned} \tag{80}$$

Thus,

$$\begin{aligned}
&\int d\hat{\mathbf{a}} Y_{LM}(\hat{\mathbf{a}}) \left(\frac{\partial^n}{\partial \lambda^n} e^{\lambda \mathbf{a} \cdot \mathbf{r}}\right)_{\lambda=0, a=1} \\
&= \int d\hat{\mathbf{a}} Y_{LM}(\hat{\mathbf{a}}) \sum_{2k+l=n} B_{kl} r^{2k+l} \sum_{m=-l}^l Y_{lm}^*(\hat{\mathbf{a}}) Y_{lm}(\hat{\mathbf{r}}) \\
&= \sum_{2k+l=n} B_{kl} r^{2k+l} \sum_{m=-l}^l \left[\int d\hat{\mathbf{a}} Y_{LM}(\hat{\mathbf{a}}) Y_{lm}^*(\hat{\mathbf{a}}) \right] Y_{lm}(\hat{\mathbf{r}}) \\
&= \sum_{2k+l=n} B_{kl} r^{2k+l} \sum_{m=-l}^l \delta_{lL} \delta_{mM} Y_{lm}(\hat{\mathbf{r}}) \\
&= B_{kL} r^{2k+L} Y_{LM}(\hat{\mathbf{r}})
\end{aligned} \tag{81}$$

with $k = (n - L)/2$.

During the integral evaluation we shall use the following form for the spatial basis functions corresponding to the $\lambda = (N, M_N, p)$ quantum numbers with $p = (-1)^N$ natural parity, which is represented by an angular prefactor in the global vector representation (GVR-ECG function):

$$\phi^{[\lambda]}(\mathbf{r}; \mathbf{A}, \mathbf{u}, K) = |\mathbf{v}|^{2K+N} Y_{NM_N}(\hat{\mathbf{v}}) \exp\left(-\frac{1}{2} \mathbf{r}^T (\mathbf{A} \otimes \mathbf{I}_3) \mathbf{r}\right), \tag{82}$$

$$= \frac{1}{B_{KN}} \int d\hat{\mathbf{e}} Y_{NM_N}(\hat{\mathbf{e}}) \left\{ \frac{\partial^{2K+N}}{\partial a^{2K+N}} g(\mathbf{r}; \mathbf{A}, a \mathbf{u} \otimes \mathbf{e}) \right\}_{a=0, |\mathbf{e}|=1}, \tag{83}$$

with the generating function

$$g(\mathbf{r}; \mathbf{A}, a \mathbf{u} \otimes \mathbf{e}) = \exp\left(-\frac{1}{2} \mathbf{r}^T (\mathbf{A} \otimes \mathbf{I}_3) \mathbf{r} + a \mathbf{u} \otimes \mathbf{e}^T \mathbf{r}\right) \tag{84}$$

and the global vector

$$\mathbf{v} = (\mathbf{u} \otimes \mathbf{e})^T \mathbf{r} = \sum_{i=1}^{n_p+1} u_i \mathbf{r}_i. \quad (85)$$

B. Spin functions

If one-particle basis functions, *e.g.*, orbitals, are employed, it is straightforward to introduce symmetry and antisymmetry for bosonic and fermionic particles by using a Hartree product and Slater determinant, respectively. However, for many-particle spatial functions, it is necessary to perform the (anti)symmetrization of the product of the spin and spatial functions explicitly using Eqs. (56) and (57). The previous subsection was about the construction of symmetry-adapted spatial functions, this subsection will introduce symmetry-adapted spin functions. By symmetry-adapted we mean that the function, $\chi^{[s]}$, is an eigenfunction of the total spin operators with the selected eigenvalues, $S_a, M_{S_a}, S_b, M_{S_b}, \dots$ for each particle type a, b, \dots :

$$\hat{S}_a^2 \chi = S_a(S_a + 1) \chi \quad (86)$$

$$\hat{S}_{a,z} \chi = M_{S_a} \chi \quad (87)$$

In most of the cases, it is appropriate to consider the different particle types independently (the positronium molecule, Ps_2 , is a notable exception). In what follows, we present examples for the explicit construction of two- and three-particle spin eigenfunctions of spin-1/2 particles.

The elementary spin functions are labelled with

$$\alpha = \sigma_{\frac{1}{2}, \frac{1}{2}}, \quad (88)$$

which is an eigenfunction of the one-particle spin-operators:

$$\begin{aligned} \hat{s}^2 \sigma_{\frac{1}{2}, \frac{1}{2}} &= \frac{1}{2} \left(1 + \frac{1}{2} \right) \sigma_{\frac{1}{2}, \frac{1}{2}} &\Rightarrow & \hat{s}^2 \alpha = \frac{3}{4} \alpha \\ \hat{s}_z \sigma_{\frac{1}{2}, \frac{1}{2}} &= \frac{1}{2} \sigma_{\frac{1}{2}, \frac{1}{2}} &\Rightarrow & \hat{s}_z \alpha = \frac{1}{2} \alpha \end{aligned} \quad (89)$$

Similarly,

$$\beta = \sigma_{\frac{1}{2}, -\frac{1}{2}}, \quad (90)$$

which is an eigenfunction of the one-particle spin-operators:

$$\begin{aligned} \hat{s}^2 \sigma_{\frac{1}{2}, -\frac{1}{2}}(1) &= \frac{1}{2} \left(1 + \frac{1}{2} \right) \sigma_{\frac{1}{2}, -\frac{1}{2}}(1) &\Rightarrow & \hat{s}^2 \beta = \frac{3}{4} \beta \\ \hat{s}_z \sigma_{\frac{1}{2}, -\frac{1}{2}}(1) &= -\frac{1}{2} \sigma_{\frac{1}{2}, -\frac{1}{2}}(1) &\Rightarrow & \hat{s}_z \beta = -\frac{1}{2} \beta. \end{aligned} \quad (91)$$

In order to construct the many-particle spin function $\Sigma_{S, M_S}(1, 2, \dots, n)$ with S and M_S total spin quantum numbers, we shall couple the elementary spin function following the rules of angular momentum coupling. First of all, for n particles the α and β functions are distributed among the particles according to the following restrictions:

$$n_\alpha + n_\beta = n \quad (92)$$

and

$$\begin{aligned} M_S &= m_{s_\alpha} n_\alpha + m_{s_\beta} n_\beta \\ &= \frac{1}{2} n_\alpha - \frac{1}{2} n_\beta. \end{aligned} \quad (93)$$

How many uncoupled n -particle basis functions are there, which contribute to $\Sigma_{S, M_S}(1, 2, \dots, n)$? Since $\Sigma_{S, M_S}(1, 2, \dots, n)$ must contain $n_\alpha = (n + 2M_S)/2$ α -type and $n_\beta = (n - 2M_S)/2$ β -type one-particle spin functions, $\sigma_{\frac{1}{2}, m_{s_\alpha}}(i)$, there is a total number of $N_S = \binom{n}{n_\alpha} = \binom{n}{n_\beta}$ uncoupled n -particle spin functions which may contribute to $\Sigma_{S, M_S}(1, 2, \dots, n)$.

In what follows, we obtain the explicit formulae for $\Sigma_{S, M_S}(1, 2, \dots, n)$ as a linear combination of the uncoupled many-particle spin functions using the Clebsch–Gordan expansion coefficients and the normalization requirement.

Two spin-1/2 particles, $\Sigma_{00}(1, 2)$ (“singlet”, $2 \cdot 0 + 1 = 1$):

$$n = 2, M_S = 0 \quad \Rightarrow \quad n_\alpha = 1, n_\beta = 1, N_S = \binom{n}{n_\alpha} = 2. \quad (94)$$

So, there are 2 uncoupled functions: 1 α -type and 1 β -type functions.

$$\begin{aligned} \Sigma_{0,0}(1, 2) &= [\sigma_{\frac{1}{2}}(1) \times \sigma_{\frac{1}{2}}(2)]_{0,0} \\ &= \langle \frac{1}{2}, \frac{1}{2}, \frac{1}{2}, -\frac{1}{2} | 0, 0 \rangle \sigma_{\frac{1}{2}, \frac{1}{2}}(1) \sigma_{\frac{1}{2}, -\frac{1}{2}}(2) \\ &\quad + \langle \frac{1}{2}, -\frac{1}{2}, \frac{1}{2}, \frac{1}{2} | 0, 0 \rangle \sigma_{\frac{1}{2}, -\frac{1}{2}}(1) \sigma_{\frac{1}{2}, \frac{1}{2}}(2) \\ &= \frac{1}{\sqrt{2}} \sigma_{\frac{1}{2}, \frac{1}{2}}(1) \sigma_{\frac{1}{2}, -\frac{1}{2}}(2) - \frac{1}{\sqrt{2}} \sigma_{\frac{1}{2}, -\frac{1}{2}}(1) \sigma_{\frac{1}{2}, \frac{1}{2}}(2) \\ &= \frac{1}{\sqrt{2}} (|\alpha\beta\rangle - |\beta\alpha\rangle) \\ &= \frac{1}{\sqrt{2}} (|\uparrow\downarrow\rangle - |\downarrow\uparrow\rangle). \end{aligned} \quad (95)$$

Two spin-1/2 particles, $\Sigma_{10}(1, 2)$ (“triplet”, $2 \cdot 1 + 1 = 3$):

$$n = 2, M_S = 0 \quad \Rightarrow \quad n_\alpha = 1, n_\beta = 1, N_S = \binom{n}{n_\alpha} = 2 \quad (96)$$

and

$$\begin{aligned} \Sigma_{1,0}(1, 2) &= [\sigma_{\frac{1}{2}}(1) \sigma_{\frac{1}{2}}(2)]_{1,0} \\ &= \langle \frac{1}{2}, \frac{1}{2}, \frac{1}{2}, -\frac{1}{2} | 1, 0 \rangle \sigma_{\frac{1}{2}, \frac{1}{2}}(1) \sigma_{\frac{1}{2}, -\frac{1}{2}}(2) \\ &\quad + \langle \frac{1}{2}, -\frac{1}{2}, \frac{1}{2}, \frac{1}{2} | 1, 0 \rangle \sigma_{\frac{1}{2}, -\frac{1}{2}}(1) \sigma_{\frac{1}{2}, \frac{1}{2}}(2) \\ &= \frac{1}{\sqrt{2}} \sigma_{\frac{1}{2}, \frac{1}{2}}(1) \sigma_{\frac{1}{2}, -\frac{1}{2}}(2) + \frac{1}{\sqrt{2}} \sigma_{\frac{1}{2}, -\frac{1}{2}}(1) \sigma_{\frac{1}{2}, \frac{1}{2}}(2) \\ &= \frac{1}{\sqrt{2}} (|\uparrow\downarrow\rangle + |\downarrow\uparrow\rangle). \end{aligned} \quad (97)$$

Three spin-1/2 particles, $\Sigma_{\frac{1}{2}, \frac{1}{2}}(1, 2, 3)$ (“doublet”, $2 \cdot 1/2 + 1 = 2$): For three spin-1/2 particles the $\Sigma_{\frac{1}{2}, \frac{1}{2}}(1, 2, 3)$ spin function has $M_S = 1/2$, and thus $n_\alpha = 2$ and $n_\beta = 1$ with $N_s = \binom{n}{n_\alpha} = \binom{n}{n_\beta} = 3$ uncoupled basis functions. Then, the total spin function expressed in terms of the uncoupled spin functions can be obtained by

evaluating

$$\Sigma_{\frac{1}{2},\frac{1}{2}}(1, 2, 3) = c_1 \left[[\sigma_{\frac{1}{2}}(1)\sigma_{\frac{1}{2}}(2)]_1 \sigma_{\frac{1}{2}}(3) \right]_{\frac{1}{2},\frac{1}{2}} + c_2 \left[[\sigma_{\frac{1}{2}}(1)\sigma_{\frac{1}{2}}(2)]_0 \sigma_{\frac{1}{2}}(3) \right]_{\frac{1}{2},\frac{1}{2}}. \quad (98)$$

The normalization condition for $\Sigma_{\frac{1}{2},\frac{1}{2}}(1, 2, 3)$ requires $c_1^2 + c_2^2 = 1$, which can be fulfilled by choosing $c_1 = \sin \vartheta_1$ and $c_2 = \cos \vartheta_1$ with $\vartheta_1 \in [-\pi/2, \pi/2]$. Then, we couple the one-particle spin functions, insert the corresponding Clebsch–Gordan coefficients, and obtain:

$$\begin{aligned} \Sigma_{\frac{1}{2},\frac{1}{2}}(1, 2, 3) &= \sin \vartheta_1 \langle 1, 0, \frac{1}{2}, \frac{1}{2} | \frac{1}{2}, \frac{1}{2} \rangle [\sigma_{\frac{1}{2}}(1)\sigma_{\frac{1}{2}}(2)]_{1,0} \sigma_{\frac{1}{2},\frac{1}{2}}(3) \\ &\quad + \sin \vartheta_1 \langle 1, 1, \frac{1}{2}, -\frac{1}{2} | \frac{1}{2}, \frac{1}{2} \rangle [\sigma_{\frac{1}{2}}(1)\sigma_{\frac{1}{2}}(2)]_{1,1} \sigma_{\frac{1}{2},-\frac{1}{2}}(3) \\ &\quad + \cos \vartheta_1 \langle 0, 0, \frac{1}{2}, \frac{1}{2} | \frac{1}{2}, \frac{1}{2} \rangle [\sigma_{\frac{1}{2}}(1)\sigma_{\frac{1}{2}}(2)]_{0,0} \sigma_{\frac{1}{2},\frac{1}{2}}(3) \\ &= \kappa_1(\vartheta_1) \sigma_{\frac{1}{2},\frac{1}{2}}(1)\sigma_{\frac{1}{2},-\frac{1}{2}}(2)\sigma_{\frac{1}{2},\frac{1}{2}}(3) \\ &\quad + \kappa_2(\vartheta_1) \sigma_{\frac{1}{2},\frac{1}{2}}(1)\sigma_{\frac{1}{2},\frac{1}{2}}(2)\sigma_{\frac{1}{2},-\frac{1}{2}}(3) \\ &\quad + \kappa_3(\vartheta_1) \sigma_{\frac{1}{2},-\frac{1}{2}}(1)\sigma_{\frac{1}{2},\frac{1}{2}}(2)\sigma_{\frac{1}{2},\frac{1}{2}}(3). \end{aligned} \quad (99)$$

where the calculation of the linear combination coefficients $\boldsymbol{\kappa}(\vartheta_1) = (\kappa_1(\vartheta_1), \kappa_2(\vartheta_1), \kappa_3(\vartheta_1))$, is left for an exercise. The final result is

$$\kappa_1(\vartheta_1) = \frac{1}{\sqrt{2}} \cos \vartheta_1 - \frac{1}{\sqrt{6}} \sin \vartheta_1 \quad (100)$$

$$\kappa_2(\vartheta_1) = \sqrt{\frac{2}{3}} \sin \vartheta_1 \quad (101)$$

$$\kappa_3(\vartheta_1) = -\frac{1}{\sqrt{2}} \cos \vartheta_1 - \frac{1}{\sqrt{6}} \sin \vartheta_1. \quad (102)$$

If there are several types of identical particles, a, b, \dots in the system, the total spin function can be written as the product of the coupled functions of each type:

$$\chi_{S,M_S} = \Sigma_{S_a,M_{S_a}}(1, \dots, n_a) \Sigma_{S_b,M_{S_b}}(1, \dots, n_b) \dots \quad (103)$$

where (S, M_S) is a collective index for $(S_a, M_{S_a}), (S_b, M_{S_b}), \dots$. Since the total spin function for any particle type a , $\Sigma_{S_a,M_{S_a}}(1, \dots, n_a)$, can be written as a linear combination of uncoupled many-particle spin functions, the χ_{S,M_S} function can also be

written in a similar way, and thus for later convenience we introduce the shorthand notation:

$$\chi_{S,M_S}(\boldsymbol{\vartheta}) = \sum_{n=1}^{N_s} \kappa_n(\boldsymbol{\vartheta}) |n\rangle_{\boldsymbol{\sigma}}, \quad (104)$$

where $|n\rangle_{\boldsymbol{\sigma}}$ denotes the product of uncoupled many-particle spin functions for each particle type, $N_s = N_{s_a} N_{s_b} \dots$, $\boldsymbol{\sigma}$ refers to the spin degrees of freedom, and $\boldsymbol{\vartheta}$ contains the free parameters if there are several “partial waves”. The value of $\kappa_n(\boldsymbol{\vartheta})$ is determined by the normalization condition, the Clebsch–Gordan coefficients, and the angular momentum coupling procedure carried out for each particle types similarly to Eqs. (95)–(102).

VI. MATRIX ELEMENTS

A matrix element of a spin-independent and permutationally invariant operator, \hat{O} with (anti)symmetrized, symmetry-adapted, $\lambda = (N, M_N, p)$ and $\varsigma = (S_a, M_{S_a}, S_b, M_{S_b}, \dots)$, spin-spatial basis function is evaluated as

$$\begin{aligned} O_{IJ}^{[\lambda, \varsigma]} &= \langle \Phi_I^{[\lambda, \varsigma]} | \hat{O} | \Phi_J^{[\lambda, \varsigma]} \rangle_{\mathbf{r}, \boldsymbol{\sigma}} \\ &= \langle \hat{\mathcal{A}}\{\phi_I^{[\lambda]} \chi_I^{[\varsigma]}\} | \hat{O} | \hat{\mathcal{A}}\{\phi_J^{[\lambda]} \chi_J^{[\varsigma]}\} \rangle_{\mathbf{r}, \boldsymbol{\sigma}} . \end{aligned} \quad (105)$$

The antisymmetrizer (which generates $N_{\text{perm}} \sim (n_p + 1)!$ elements) can be eliminated from the bra by using its quasi-idempotent property, $\hat{\mathcal{A}}\hat{\mathcal{A}} = (N_{\text{perm}})^{1/2}\hat{\mathcal{A}}$:

$$\begin{aligned} O_{IJ}^{[\lambda, \varsigma]} &= \sum_{p=1}^{N_{\text{perm}}} \varepsilon_p \langle \phi_I^{[\lambda]} \chi_I^{[\varsigma]} | \hat{O} | \hat{P}_p \{\phi_J^{[\lambda]} \chi_J^{[\varsigma]}\} \rangle_{\mathbf{r}, \boldsymbol{\sigma}} \\ &= \sum_{p=1}^{N_{\text{perm}}} \varepsilon_p \langle \chi_I^{[\varsigma]} | \hat{P}_p \chi_J^{[\varsigma]} \rangle_{\boldsymbol{\sigma}} \langle \phi_I^{[\lambda]} | \hat{O} | \hat{P}_p \phi_J^{[\lambda]} \rangle_{\mathbf{r}} \\ &= \sum_{p=1}^{N_{\text{perm}}} c_{IJ_p}^{[\varsigma]} O_{IJ_p}^{[\lambda]} \end{aligned} \quad (106)$$

where the spin and the spatial integrals are separated to

$$c_{IJ_p}^{[\varsigma]} = \varepsilon_p \langle \chi_I^{[\varsigma]} | \hat{P}_p \chi_J^{[\varsigma]} \rangle_{\boldsymbol{\sigma}} \quad (107)$$

$$O_{IJ_p}^{[\lambda]} = \langle \phi_I^{[\lambda]} | \hat{O} | \hat{P}_p \phi_J^{[\lambda]} \rangle_{\mathbf{r}} . \quad (108)$$

Since the operator is spin-independent, the calculation of $c_{IJ_p}^{[\varsigma]}$ requires simple algebra. The calculation of $O_{IJ_p}^{[\lambda]}$ is less trivial and certainly depends on \hat{O} , which is, in the present discussion, the identity, \hat{I} , the kinetic, \hat{T} , or the potential energy, \hat{V} , operator. For the full calculation of the analytic matrix elements see the *Recommended Literature*. In what follows, we highlight the most important steps of the derivation.

First of all, a matrix element of an operator \hat{O} is written using the exponential generator integral for the angular prefactor, Eq. (83),

$$\begin{aligned} & \langle \phi^{[\lambda]}(\mathbf{r}; \mathcal{A}, \mathbf{u}, K) | \hat{O} | \phi^{[\lambda]}(\mathbf{r}; \mathcal{A}', \mathbf{u}', K') \rangle_{\mathbf{r}} \\ &= \frac{1}{B_{KN} B_{K'N}} \int d\hat{\mathbf{e}} \int d\hat{\mathbf{e}}' \theta_{NMN}^*(\hat{\mathbf{e}}) \theta_{NMN}(\hat{\mathbf{e}}') \\ & \times \left\{ \frac{\partial^{2K+L}}{\partial a^{2K+L}} \frac{\partial^{2K'+L}}{\partial a'^{2K'+L}} \langle g(\mathbf{r}; \mathcal{A}, s(a, \mathbf{u}, \mathbf{e})) | \hat{O} | g(\mathbf{r}; \mathcal{A}', s'(a', \mathbf{u}', \mathbf{e}')) \rangle_{\mathbf{r}} \right\}_{a=a'=0, |\mathbf{e}|=|\mathbf{e}'|=1}, \end{aligned} \quad (109)$$

which is evaluated according to the following steps

1. Calculation of the integral with respect to the spatial coordinates \mathbf{r} and the generating functions (floating ECGs) is usually straightforward for the most common operators

$$I_{O,1}(s, s') = \langle g(\mathbf{r}; \mathcal{A}, s) | \hat{O} | g(\mathbf{r}; \mathcal{A}', s') \rangle_{\mathbf{r}} \quad (110)$$

2. The differentiation of the integral in Eq. (110) is carried out for $\partial^{2K+N}/\partial a^{2K+N}$ and $\partial^{2K'+N}/\partial a'^{2K'+N}$ and the result is expressed in terms of polynomials of scalar products, $\mathbf{e}^T \mathbf{e}'$,

$$I_{O,2}^{[(N)]}(\mathbf{e}, \mathbf{e}') = \left\{ \frac{\partial^{2K+N}}{\partial a^{2K+N}} \frac{\partial^{2K'+N}}{\partial a'^{2K'+N}} I_{O,1}(s(a, \mathbf{u}, \mathbf{e}), s'(a', \mathbf{u}', \mathbf{e}')) \right\}_{a=a'=0, |\mathbf{e}|=|\mathbf{e}'|=1} \quad (111)$$

3. In the last step the angular integral is calculated:

$$I_{O,3}^{[\lambda=(N, M_N, (-1)^N)]} = \frac{1}{B_{KL} B_{K'L}} \int d\hat{\mathbf{e}} \int d\hat{\mathbf{e}}' Y_{NMN}^*(\hat{\mathbf{e}}) Y_{NMN}(\hat{\mathbf{e}}') I_{O,2}^{[(N)]}(\mathbf{e}, \mathbf{e}'). \quad (112)$$

During the course of the evaluation of the angular integral, we make use of the following identity of spherical harmonics

$$(\mathbf{e}^T \mathbf{e}')^k = \sum_{\substack{l=0 \\ [(k-l)/2 \in \mathbb{N}_0]}}^k B_{\frac{k-l}{2}, l} \sum_{m=-l}^l Y_{lm}^*(\hat{\mathbf{e}}) Y_{lm}(\hat{\mathbf{e}}) . \quad (113)$$

which is for $k = 1$

$$\mathbf{e}^T \mathbf{e}' = \frac{4\pi}{3} \sum_{m=-1}^1 Y_{1m}^*(\hat{\mathbf{e}}) Y_{1m}(\hat{\mathbf{e}}) . \quad (114)$$

Concerning practical applications, it is important to note that for large $(2K + L) > 4$ values special care must be taken during the course of the implementation of the analytic formulae in order to avoid numerical instabilities in finite number representation (double precision in Fortran). To ensure numerical stability we introduce a so-called “quasi-normalization” of the basis functions, which allows us to cancel some problematic terms. We call the normalization with respect to the spatial function,

$$\Phi^{[\lambda, s]} = (\langle \phi^{[\lambda]} | \phi^{[\lambda]} \rangle_{\mathbf{r}})^{-1/2} \hat{\mathcal{A}}\{\phi^{[\lambda]} \chi^{[s]}\} , \quad (115)$$

quasi-normalization. In a computer implementation it may also be useful to rely on a logarithmic evaluation of products and fractions, *e.g.*,

$$(a \cdot b)/(c \cdot d) = \text{sign}(ab/cd) \cdot 10^{(\lg a + \lg b - \lg c - \lg d)} \quad (116)$$

to calculate small numbers as ratios and products of large ones. Furthermore, it is possible to factor out a term, which appears in the integrals,

$$F_{KL} = \sum_{m=0}^K \frac{2^m (L + m + 1)!}{(K - m)! (K - m)! m! (2L + 2m + 2)!} , \quad (117)$$

which is pre-calculated with infinite precision arithmetics (*e.g.*, using the *Mathematica* program) for a series of K and L integer values. These numbers are stored in a file and are read in by the Fortran program at the beginning of each computation.

VII. COMPUTATION OF EIGENSTATES

In the previous sections we outlined how the matrix representation of the Hamiltonian is constructed in a finite basis set (with N_b basis functions). It is often convenient to use a basis set which is not orthonormal (such as the ECG-GVR functions) and thus, we have to consider the generalized eigenproblem with a non-diagonal overlap matrix, $\mathbf{S} \neq \mathbf{I}$:

$$\mathbf{H}\mathbf{c} = E\mathbf{S}\mathbf{c}, \quad (118)$$

where \mathbf{H} and $\mathbf{S} \in \mathbb{R}^{N_b \times N_b}$ are real and symmetric matrices. In order to be able to use standard direct eigensolver routines (*e.g.*, LAPACK), we need to transform this equation as follows.

We assume that the basis set is linearly independent, and multiply Eq. (118) with $\mathbf{S}^{-1/2}$ from the left

$$\mathbf{S}^{-\frac{1}{2}}\mathbf{H}\mathbf{c} = E\mathbf{S}^{\frac{1}{2}}\mathbf{c} \quad (119)$$

$$\mathbf{S}^{-\frac{1}{2}}\mathbf{H}\mathbf{S}^{-\frac{1}{2}}\mathbf{S}^{\frac{1}{2}}\mathbf{c} = E\mathbf{S}^{\frac{1}{2}}\mathbf{c} \quad (120)$$

$$\mathbf{H}'\mathbf{c}' = E\mathbf{c}' \quad (121)$$

with

$$\mathbf{H}' = \mathbf{S}^{-\frac{1}{2}}\mathbf{H}\mathbf{S}^{-\frac{1}{2}} \quad (122)$$

and

$$\mathbf{c}' = \mathbf{S}^{\frac{1}{2}}\mathbf{c} \quad \Rightarrow \quad \mathbf{c} = \mathbf{S}^{-\frac{1}{2}}\mathbf{c}'. \quad (123)$$

A few comments are collected as follows.

- Note that the transformation in Eqs. (119)–(121) is related to Löwdin's (symmetric) orthogonalization (which is different from the Gram–Schmidt orthogonalization scheme).

- If there is a linear dependence within the basis set, there are $\lambda_i = 0$ eigenvalue(s) of the \mathbf{S} overlap matrix.
- Note that in finite precision arithmetics, near linear dependencies are also destructive, *i.e.*, when there are $\lambda_i \sim 10^{-14}$, which is almost zero in the commonly used 8-byte representation of real numbers. In this case, Lödwin’s generalized orthogonalization scheme may be adopted, which allows us to carry out a transformation similar to Eqs. (119)–(121) but neglecting the near-linear dependent part of the basis space. Alternatively, a better parameterization of the basis set ensures to avoid near linear dependencies.

a. The stabilization method In a series of variational basis representation (VBR) computations, we obtain approximations to the discrete eigenvalues of the Hamiltonian, which converge from above to the exact eigenvalues (ensured by the variational principle). In addition, by computing not only the few lowest-energy eigenvalues, we may observe the onset of the dissociation threshold and a VBR representation of continuum states. Beyond the dissociation threshold, we may observe energy intervals with an increased density of states, which correspond to quasi-bound states with a finite lifetime (although in this regime the variational principle is not applicable). (\Rightarrow Figure) In practice, long-lived resonances can be observed in a series of VBR computations by noticing the stabilization of an energy window within the continuum regime over a series of computations.

b. Complex coordinate rotation method In an alternative mathematical description, in which we choose to scale the physical distances by a complex number, $r \rightarrow re^{i\vartheta}$, and use VBR for the scaled Hamiltonian leads to a complex symmetric eigenproblem.

$$\hat{H} = \hat{T} + \hat{V} \quad \rightarrow \quad \hat{H}(\vartheta) = e^{-2i\vartheta}\hat{T} + e^{-i\vartheta}\hat{V}. \quad (124)$$

The corresponding matrix equation is written as

$$\tilde{\mathbf{H}}(\vartheta)\tilde{\mathbf{c}}_i(\vartheta) = \mathcal{E}_i(\vartheta)\mathbf{S}\tilde{\mathbf{c}}_i(\vartheta), \quad (125)$$

which, similarly to its real analogue, Eq. (118), is transformed to

$$\tilde{\mathbf{H}}'(\vartheta)\tilde{\mathbf{c}}'_i(\vartheta) = \mathcal{E}_i(\vartheta)\tilde{\mathbf{c}}'_i(\vartheta) \quad (126)$$

with

$$\begin{aligned} \tilde{\mathbf{H}}'(\vartheta) &= e^{-2i\vartheta} \mathbf{S}^{-1/2} \mathbf{T} \mathbf{S}^{-1/2} + e^{-i\vartheta} \mathbf{S}^{-1/2} \mathbf{V} \mathbf{S}^{-1/2} \\ &= \cos(2\vartheta) \mathbf{T}' + \cos(\vartheta) \mathbf{V}' - i(\sin(2\vartheta) \mathbf{T}' + \sin(\vartheta) \mathbf{V}'). \end{aligned} \quad (127)$$

The complex symmetric eigenproblem, Eq. (126), is solved using LAPACK library routines [1], and the stabilization point, $\mathcal{E} = (E, -\Gamma/2)$ with the E energy and Γ width (the lifetime is $\tau = \hbar/\Gamma$), on the complex energy plane is identified visually.

The eigenvalues of the scaled Hamiltonian lie on the complex plane and correspond to bound and resonance states of the original operator. (\Rightarrow Figure) For the eigenvalues of this complex Hamiltonian, there are generalizations for the real variational principle, which ensure their stationary property with respect to the completeness of the basis set and the scaling angle, ϑ . The complex variational principle(s) is however less practical for the parameterization of the basis set than their real analogue.

VIII. PARAMETERIZATION OF THE BASIS FUNCTIONS

1. *Non-linear parameterization strategy*

a. Parameter selection The nonlinear parameters for each basis function are selected and optimized based on the variational principle, which translates in practice to the simple rule: the lower the energy, the better the parameter set. The parameter selection is carried in a stochastic manner, in which new basis functions are generated randomly one after the other. Trial values for the parameters of the spatial basis functions, Eq. (83), K , u_i , $\ln \alpha_{ij}$, are drawn from discrete uniform, continuous uniform, and normal distributions, respectively. The optimal parameters of each distribution are estimated from short exploratory computations. Due to the one-by-one generation of the basis functions, the updated eigenvalues can be evaluated very efficiently using the known eigenvalues and eigenvectors corresponding to the old basis set, and this allows for a rapid assessment of a trial parameter set.

b. Refinement The refinement of the basis-function parameters generated by the stochastic variational method is necessary if very accurate solutions are required. Similarly to the enlargement of the basis set, the basis functions are refined one after the other using the fast eigenvalue update algorithm, which is used also for the selection of a new basis function from a set of randomly generated trials. Refined parameters can be found by random walk or using the Powell method [2] started from the originally selected parameters for each basis function. The random-walk refinement can be used to adjust the K integer value (for which the Powell method is not applicable), however in practice it is usually sufficient to generate K from a discrete uniform distribution spread over a pre-optimized interval and to refine only the continuous variables, u_i and α_{ij} by the Powell method. During the course of and at the end of the enlargement of the basis set, every basis function is refined in repeated cycles.

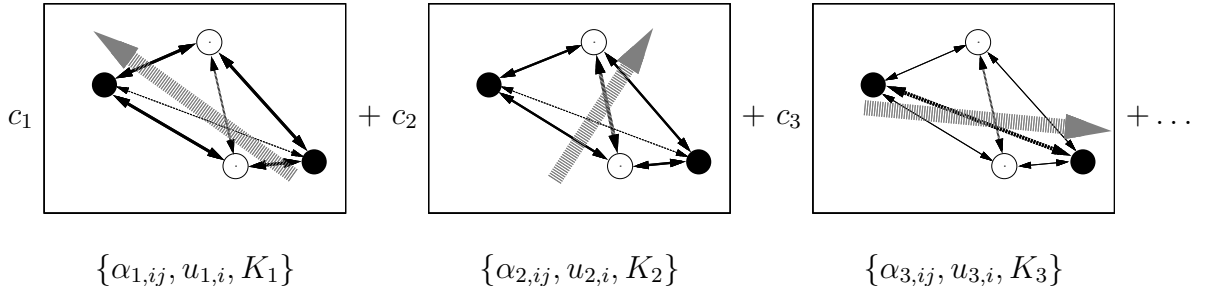
2. *Parameterization strategy for resonances*

Due to the lack of any practical approach relying on the complex variational principle to select and optimize the non-linear parameters of the basis functions,

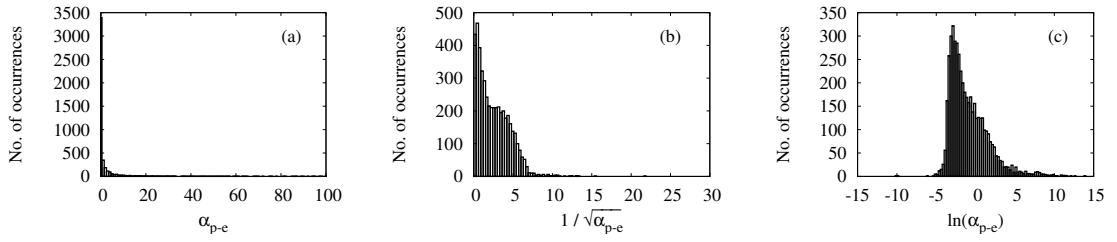
we relied on the random generation of the parameters from some broad parameter intervals. In addition, we have devised a parameter-transfer approach:

$$\Psi^{(A')} = \sum_{I=1}^{N_b} c_I \Phi_I^{(A')}[\mathcal{P}_I(A)] \quad (128)$$

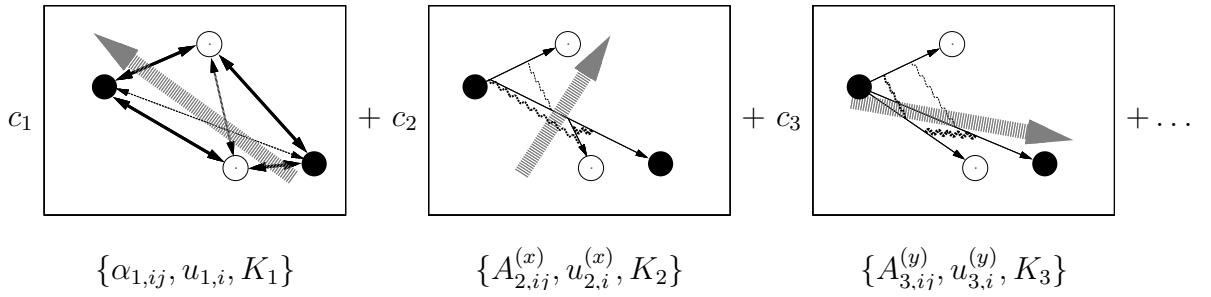
in which a parameter set optimized based on the real variational principle for bound states with one set of input parameters is transferred to a computation with other input parameters (*e.g.*, different quantum numbers). Note that the spatial symmetries of a basis function are determined by the quantum numbers, Eq. (82), and in this sense, the parameters K , u_i , and \mathbf{A} , are transferable.



(a) Non-linear parameters of the basis functions.



(b) Sampling–importance resampling for the parameter generation.



(c) Multi-channel (multi-coordinate) optimization of the non-linear parameters.

FIG. 2: Parameterization of the basis functions

IX. VARIATIONAL RESULTS FOR FEW-PARTICLE SYSTEMS

A. Atomic systems

1. ${}^7\text{Li} = \{{}^7\text{Li}^{3+}, e^-, e^-, e^-\}$

TABLE I: Calculated energy levels of ${}^7\text{Li} = \{{}^7\text{Li}^{3+}, e^-, e^-, e^-\}$.

| N ^a | p ^a | S_e ^a | E ^b | η ^c | $\delta E / \mu E_h$ ^d | Ref. |
|------------------|------------------|--------------------|------------------|---------------------|-----------------------------------|--------|
| 0 | 1 | 1/2 | -7.477 451 901 | $1.3 \cdot 10^{-9}$ | -0.029 | [3] |
| 1 | -1 | 1/2 | -7.409 557 349 | $8.8 \cdot 10^{-9}$ | -0.410 | [4] |
| 2 | 1 | 1/2 | -7.334 926 959 | $1.1 \cdot 10^{-9}$ | -0.347 | [5, 6] |

^a N : quantum number of the total angular momentum without the spins; p : parity; S_e : total spin quantum number of the electrons.

^b $m_{7\text{Li}^{3+}}/m_{e^+} = 12\,786.393$ The wave functions were optimized as a linear combination of $N_b = 1\,500$ basis functions and the exponents of the polynomial prefactors were $2K = 0$ or 2, selected randomly.

^c $\eta = |1 + \langle \Psi | \hat{V} | \Psi \rangle / (2 \langle \Psi | \hat{T} | \Psi \rangle)|$.

^d $\delta E = E(\text{Ref.}) - E$.

B. Positron-electron systems

1. $Ps^- = \{e^+, e^-, e^-\}$

parameterization of the basis functions:

- minimization of the energy
- random generation of parameters, sampling-importance resampling

TABLE II: Identified bound- and resonance-state energies and resonance widths, in E_h , of $Ps^- = \{e^-, e^-, e^+\}$.^a

| (N, p, S_-) ^b | $\text{Re}(\mathcal{E})$ ^c | $\Gamma/2$ ^c | $\text{Re}(\mathcal{E}_{\text{Ref}})$ ^c | $\Gamma_{\text{Ref}}/2$ ^c | Ref. |
|---|---------------------------------------|-------------------------|--|--------------------------------------|------|
| $(0, +1, 0)$ | $-0.262\ 005\ 070$ ^d | 0 ^d | $-0.262\ 005\ 070$ | 0 | [7] |
| $E(\text{Ps}(n=1)) = -0.25$ (lowest dissociation threshold) | | | | | |
| $(0, +1, 0)$ | $-0.076\ 030\ 455$ | $2.152 \cdot 10^{-5}$ | $-0.076\ 030\ 442$ | $2.151\ 7 \cdot 10^{-5}$ | [8] |
| $(0, +1, 0)$ | $-0.063\ 649\ 173$ | $4.369 \cdot 10^{-6}$ | $-0.063\ 649\ 175$ | $4.339\ 3 \cdot 10^{-6}$ | [8] |
| $(0, +1, 0)$ | $-0.062\ 609$ | $2.5 \cdot 10^{-5}$ | $-0.062\ 550$ | $5.0 \cdot 10^{-7}$ | [9] |
| $E(\text{Ps}(n=2)) = -0.062\ 5$ | | | | | |
| $(0, +1, 0)$ | $-0.035\ 341\ 850$ | $3.730 \cdot 10^{-5}$ | $-0.035\ 341\ 885$ | $3.732\ 9 \cdot 10^{-5}$ | [8] |
| $(0, +1, 0)$ | $-0.029\ 845\ 700$ | $2.781 \cdot 10^{-5}$ | $-0.029\ 846\ 146$ | $2.635\ 6 \cdot 10^{-5}$ | [8] |
| $(0, +1, 0)$ | $-0.028\ 271$ | $1.8 \cdot 10^{-5}$ | $-0.028\ 200$ | $7.5 \cdot 10^{-6}$ | [9] |
| $E(\text{Ps}(n=3)) = -0.027\ \dot{7}$ | | | | | |
| $(0, +1, 0)$ | $-0.020\ 199\ 000$ | $8.800 \cdot 10^{-5}$ | $-0.020\ 213\ 921$ | $6.502\ 6 \cdot 10^{-5}$ | [8] |
| $E(\text{Ps}(n=1)) = -0.25$ (lowest dissociation threshold) | | | | | |
| $(0, +1, 1)$ | $-0.063\ 537\ 352$ | $2.132 \cdot 10^{-9}$ | $-0.063\ 537\ 354$ | $1.570\ 0 \cdot 10^{-9}$ | [8] |
| $(0, +1, 1)$ | $-0.062\ 591$ | $2.6 \cdot 10^{-7}$ | $-0.062\ 550$ | $2.5 \cdot 10^{-10}$ | [9] |
| $E(\text{Ps}(n=2)) = -0.062\ 5$ | | | | | |
| $(0, +1, 1)$ | $-0.029\ 369\ 870$ | $1.300 \cdot 10^{-7}$ | $-0.029\ 370\ 687$ | $9.395\ 0 \cdot 10^{-8}$ | [8] |
| $(0, +1, 1)$ | $-0.028\ 21$ | $1.9 \cdot 10^{-5}$ | $-0.028\ 05$ | $5.0 \cdot 10^{-8}$ | [9] |
| $E(\text{Ps}(n=3)) = -0.027\ \dot{7}$ | | | | | |
| $(0, +1, 1)$ | $-0.017\ 070\ 800$ | $6.710 \cdot 10^{-6}$ | $-0.017\ 101\ 172$ | $3.560\ 9 \cdot 10^{-7}$ | [9] |

^a The dissociation threshold energies, in E_h , accessible for both the $S_- = 0$ and 1 states are $E(\text{Ps}(1)) = -1/4 = -0.25$, $E(\text{Ps}(2)) = -1/16 = -0.062\ 5$, and $E(\text{Ps}(3)) = -1/36 = -0.027\ \dot{7}$.

^b N, p , and S_- : total spatial angular momentum quantum number, parity, and total spin quantum number of the electrons, respectively.

^c $\text{Re}(\mathcal{E})$ and Γ : resonance energy and width with $\Gamma/2 = -\text{Im}(\mathcal{E})$.

^d Bound state.

$$2. \quad Ps_2 = \{e^+, e^+, e^-, e^-\}$$

parameterization of the basis functions:

- minimization of the energy
- random generation of parameters, sampling-importance resampling

TABLE III: Identified bound- and resonance-state energies and resonance widths, in E_h , of $Ps_2 = \{e^-, e^-, e^+, e^+\}$.^a

| (N, p, c) ^b | (S_-, S_+) ^c | $\text{Re}(\mathcal{E})$ ^d | $\Gamma/2$ ^d | $\text{Re}(\mathcal{E}_{\text{Ref}})$ ^d | $\Gamma_{\text{Ref}}/2$ ^d | Ref. |
|--------------------------|---------------------------|---------------------------------------|-------------------------|--|--------------------------------------|------|
| (0, +1, +1) | (0, 0) | -0.516 003 789 741 ^e | 0 ^e | -0.516 003 790 416 | 0 | [10] |
| (0, +1, +1) | (0, 0) | -0.329 38 | $3.03 \cdot 10^{-3}$ | -0.329 4 | $3.1 \cdot 10^{-3}$ | [11] |
| (0, +1, +1) | (0, 0) | -0.291 7 | $2.5 \cdot 10^{-3}$ | -0.292 4 | $1.95 \cdot 10^{-3}$ | [11] |
| (0, +1, -1) | (0, 0) | -0.314 677 072 ^e | 0 ^e | -0.314 673 3 | 0 | [11] |
| (0, +1, -1) | (0, 0) | -0.289 789 3 | $7.7 \cdot 10^{-5}$ | -0.289 76 | $7 \cdot 10^{-5}$ | [11] |
| (0, +1, -1) | (0, 0) | -0.279 25 | $2.3 \cdot 10^{-4}$ | -0.279 13 | $1 \cdot 10^{-4}$ | [11] |
| (0, +1, +1) | (1, 1) | -0.277 2 | $5.4 \cdot 10^{-4}$ | -0.276 55 | $1.55 \cdot 10^{-4}$ | [11] |
| (0, +1, -1) | (1, 1) | -0.309 0 | $5.7 \cdot 10^{-3}$ | -0.308 14 | $1.2 \cdot 10^{-4}$ | [11] |
| (0, +1, -1) | (1, 1) | -0.273 3 | $2.3 \cdot 10^{-3}$ | -0.273 6 | $8.5 \cdot 10^{-4}$ | [11] |
| (0, +1, ± 1) | (1, 0)/(0, 1) | -0.330 287 505 ^e | 0 ^e | -0.330 276 81 | 0 | [11] |
| (0, +1, ± 1) | (1, 0)/(0, 1) | -0.294 3 | $3.1 \cdot 10^{-3}$ | -0.293 9 | $2.15 \cdot 10^{-3}$ | [11] |
| (0, +1, ± 1) | (1, 0)/(0, 1) | -0.282 | $2 \cdot 10^{-3}$ | -0.282 2 | $8.5 \cdot 10^{-4}$ | [11] |

^a For the five symmetry blocks with different (N, p, c) quantum numbers and (S_-, S_+) labels the lowest accessible thresholds are $Ps(1S)+Ps(1S)$, $Ps(1S)+Ps(2P)$, $Ps(1S)+Ps(2P)$, $Ps(1S)+Ps(1S)$, $Ps(1S)+Ps(2S,2P)$, respectively [12]. The corresponding energies, in E_h , are $E(Ps(1) + Ps(1)) = -1/2 = -0.5$ and $E(Ps(1) + Ps(2)) = -5/16 = -0.312 5$. (The black and gray coloring is used to help the orientation.)

^b N, p , and c : total spatial angular momentum quantum number, parity, and charge conjugation quantum number, respectively.

^c S_- and S_+ : total spin quantum number for the electrons and the positrons, respectively. In the last symmetry block, $(S_-, S_+) = (0, 1)$ and $(S_-, S_+) = (1, 0)$, are not good quantum numbers because these spin states are coupled due to the charge-conjugation symmetry of the Hamiltonian.

^d $\text{Re}(\mathcal{E})$ and Γ : resonance energy and width with $\Gamma/2 = -\text{Im}(\mathcal{E})$.

^e Bound states.

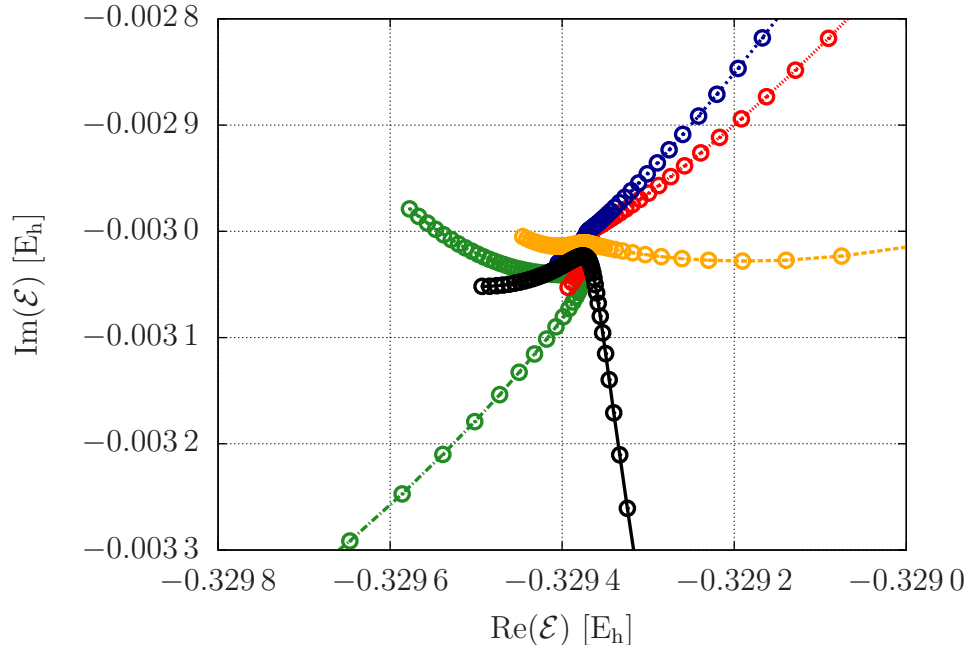


FIG. 3: Localization of the parameters for the lowest-energy resonance state of Ps_2 with $N = 0$, $p = +1$, $c = +1$, and $S_- = 0$, $S_+ = 0$. The stabilization of the trajectories with respect to the rotation angle (circles) and the basis functions (colors) is shown. The stabilization point is located at $(\text{Re}(\mathcal{E}), \text{Im}(\mathcal{E})) = (-0.329\ 38, -0.003\ 03) E_h$.

C. Molecular systems

1. $H_2^+ = \{p^+, p^+, e^-\}$

parameterization of the basis functions:

- polynomial prefactors
- sampling-importance resampling, refinement with Powell's method

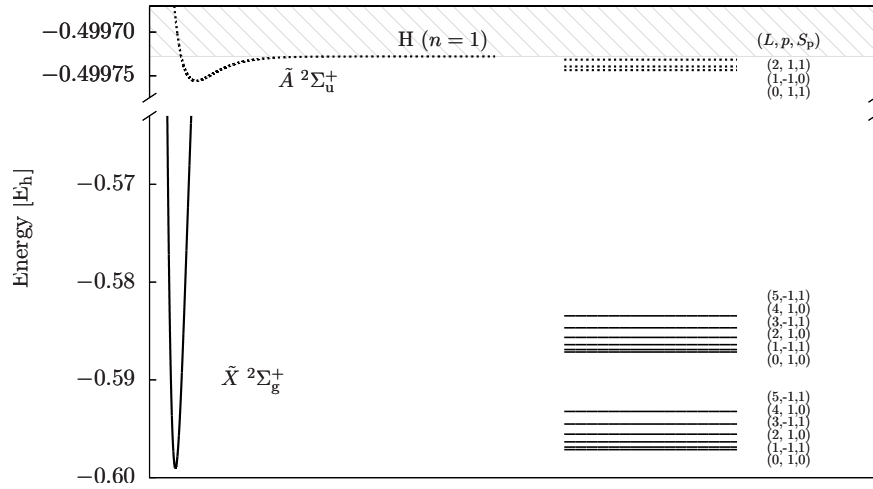


FIG. 4: Illustration of the computed pre-BO energy levels of $H_2^+ = \{p^+, p^+, e^-\}$. For comparison the BO potential energy curves are also shown (on the left).

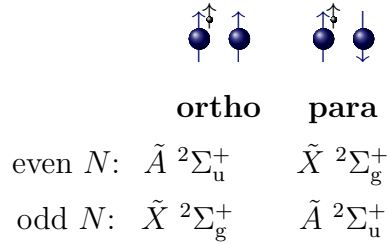


TABLE IV: Energy levels, dissociation energies (examples) of $H_2^+ = \{p^+, p^+, e^-\}$.

| N | p | S_p | E / E_h | D / cm^{-1} | Assignment |
|-----|-----|-------|-------------------|----------------------|---|
| 2 | 1 | 1 | -0.499 731 516(7) | 0.807(1) | $\tilde{A} \ ^2\Sigma_u^+, v = 0$; ortho |
| ... | | | | | |
| 0 | 1 | 0 | -0.597 139 060(4) | 21 379.290(2) | $\tilde{X} \ ^2\Sigma_g^+, v = 0$; para |

2. $H_2 = \{p^+, p^+, e^-, e^-\}$

parameterization of the basis functions:

- polynomial prefactors
- sampling-importance resampling, refinement with Powell’s method

TABLE V: Assessment of the basis set parameterization: the lowest-lying bound-state energies.

| (N, p, S_p, S_e) ^a | E/E_h ^b | $\Delta E_{\text{Ref}}/\mu E_h$ ^c | Ref. Assignment ^d |
|---------------------------------|-------------------------------|--|------------------------------|
| (0, +1, 0, 0) | -1.164 025 030 | -0.000 6 [13] | $X \ ^1\Sigma_g^+$ |
| (1, -1, 1, 0) | -1.163 485 171 | -0.001 4 [13] | $X \ ^1\Sigma_g^+$ |
| (2, +1, 0, 0) | -1.162 410 408 | -0.001 9 [13] | $X \ ^1\Sigma_g^+$ |
| (0, +1, 1, 0) | -0.753 027 186 | 0.135 4 [14] | $B \ ^1\Sigma_u^+$ |
| (1, -1, 0, 0) | -0.752 850 233 | 0.834 2 [14] | $B \ ^1\Sigma_u^+$ |
| (1, +1, 1, 0) | -0.752 498 022 | 0.918 8 [14] | $B \ ^1\Sigma_u^+$ |
| (0, +1, 0, 1) | -0.730 825 193 | -0.006 9 [15] | $a \ ^3\Sigma_g^+$ |
| (1, -1, 1, 1) | -0.730 521 418 | 0.008 0 [15] | $a \ ^3\Sigma_g^+$ |
| (2, +1, 0, 1) | -0.729 916 268 | 0.047 9 [15] | $a \ ^3\Sigma_g^+$ |
| (0, +1, 1, 1) | [-0.999 450 102] ^e | [-5.578] ^f | $b \ ^3\Sigma_u^+$ |
| (1, -1, 0, 1) | [-0.999 445 835] ^e | [-9.844] ^f | $b \ ^3\Sigma_u^+$ |
| (2, +1, 1, 1) | [-0.999 439 670] ^e | [-16.010] ^f | $b \ ^3\Sigma_u^+$ |

^a N : total spatial angular momentum quantum number; p : parity, $p = (-1)^N$; S_p and S_e : total spin quantum numbers for the protons and the electrons, respectively.

^b E : the energy obtained with the largest parameter set, \mathcal{P}_L , used in this study corresponding to 15 500 basis functions for each set of quantum numbers. The proton-electron ratio was $m_p/m_e = 1\,836.152\,672\,47$ [16].

^c $\Delta E_{\text{Ref}} = E_{\text{Ref}} - E$ with E_{Ref} being the best available theoretical energy value in the literature.

^d Born–Oppenheimer electronic state label. Each energy level given here can be assigned to the lowest-energy vibrational level of the electronic state.

^e The lowest-energy eigenvalue of the Hamiltonian obtained for the given set of quantum numbers.

^f The non-relativistic energy of two ground-state hydrogen atoms, $E(\text{H}(1) + \text{H}(1)) = -0.999\,455\,679 E_h$, was used as reference.

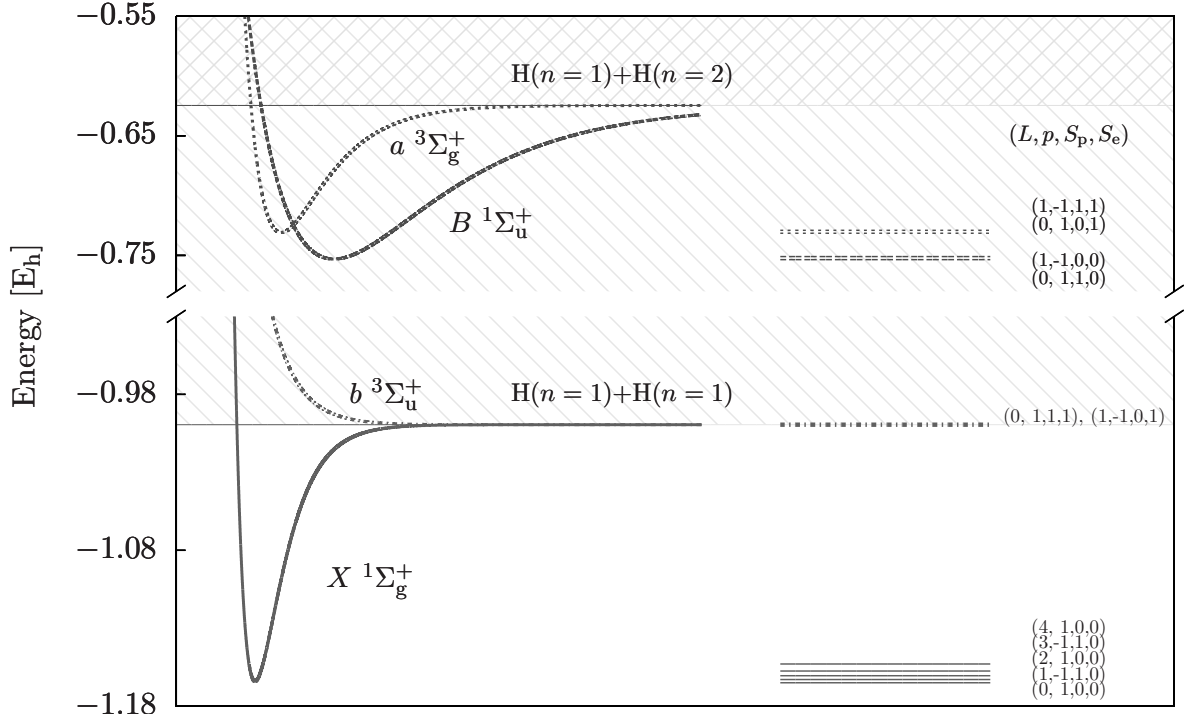


FIG. 5: Illustration of the computed pre-BO levels of $\text{H}_2 = \{\text{p}^+, \text{p}^+, \text{e}^-, \text{e}^-\}$. For comparison the BO potential energy curves are also shown (on the left).

| | singlet, para | triplet, ortho | singlet, ortho | triplet, para |
|-----------------------|--------------------|--------------------|--------------------|--------------------|
| even N , $p = +1$: | $X \ ^1\Sigma_g^+$ | $b \ ^3\Sigma_u^+$ | $B \ ^1\Sigma_u^+$ | $a \ ^3\Sigma_g^+$ |
| odd N , $p = -1$: | $B \ ^1\Sigma_u^+$ | $a \ ^3\Sigma_g^+$ | $X \ ^1\Sigma_g^+$ | $b \ ^3\Sigma_u^+$ |

According to the spatial and permutational symmetry properties of the H_2 molecule, there are four different blocks with natural parity

B1: “ $X \ ^1\Sigma_g^+$ block”: $N \geq 0$, $p = (-1)^N$, $S_p = (1 - p)/2$, $S_e = 0$;

B2: “ $B \ ^1\Sigma_u^+$ block”: $N \geq 0$, $p = (-1)^N$, $S_p = (1 + p)/2$, $S_e = 0$;

B3: “ $a \ ^3\Sigma_g^+$ block”: $N \geq 0$, $p = (-1)^N$, $S_p = (1 - p)/2$, $S_e = 1$;

B4: “ $b \ ^3\Sigma_u^+$ block”: $N \geq 0$, $p = (-1)^N$, $S_p = (1 + p)/2$, $S_e = 1$,

which can be accessed in independent runs of our computer program using basis functions with the appropriate quantum numbers.

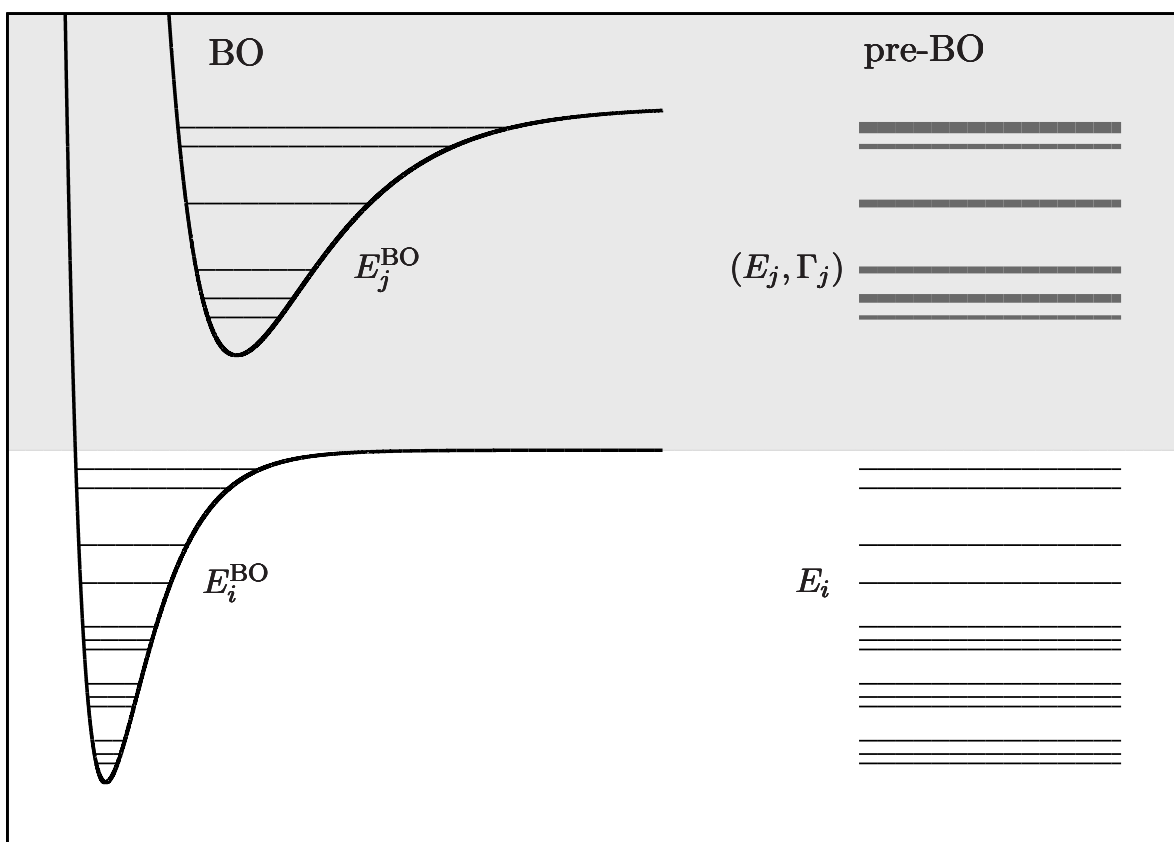


FIG. 7: **Rovibrational levels of excited electronic states in pre-BO theory:** The ladder structure of the pre-Born–Oppenheimer (pre-BO) energy levels (right). The left of the figure visualizes the rovibrational states corresponding to their respective potential energy surfaces in the Born–Oppenheimer (BO) approximation. While in the BO picture, the rovibrational states corresponding to the excited electronic state are bound states, they appear as resonances in the full pre-BO treatment. [Reprinted with permission from E. Mátyus, *J. Phys. Chem. A* 117, 7195 (2013). Copyright 2013 American Chemical Society.]

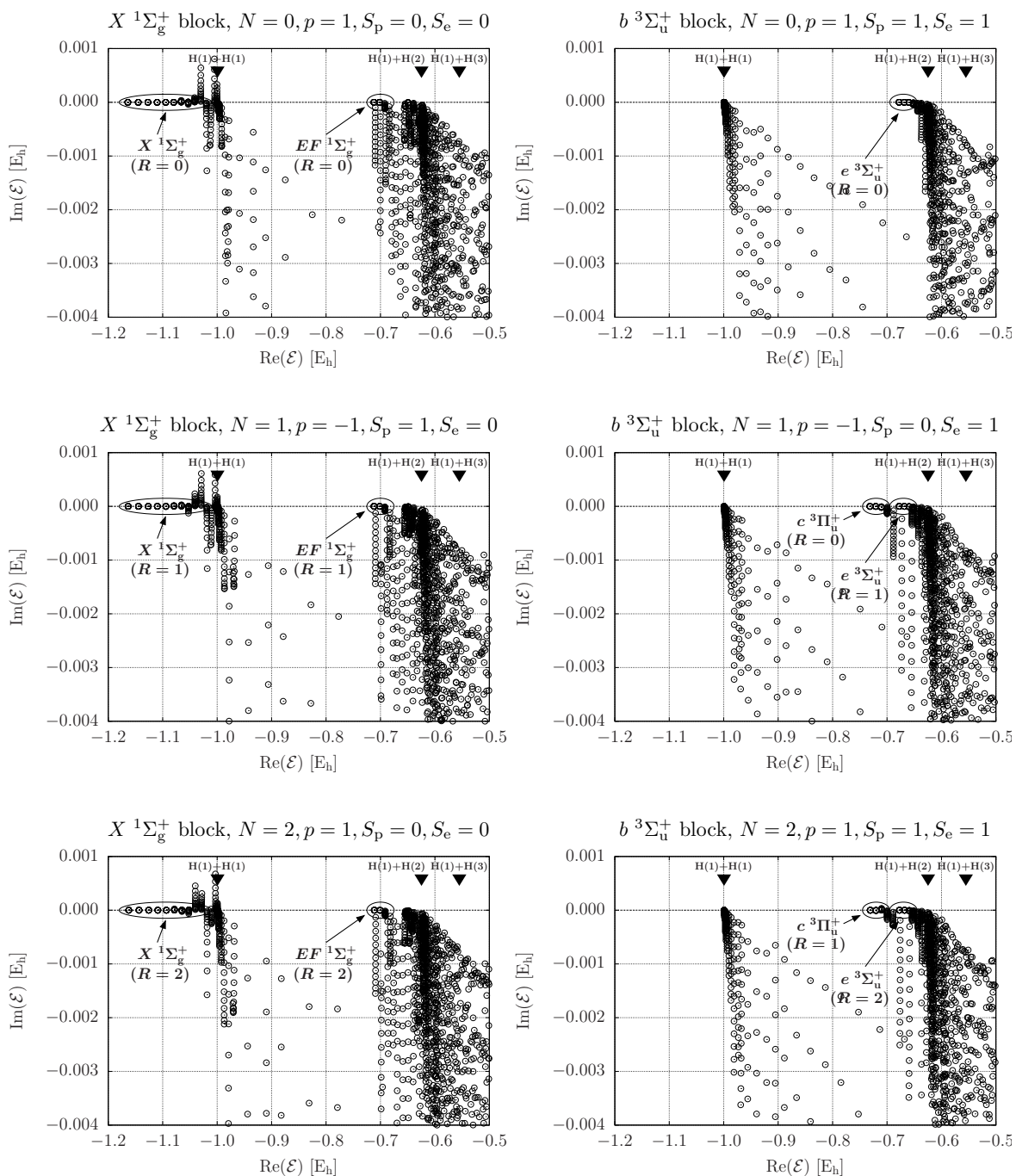


FIG. 8: Part of the spectrum of the complex scaled Hamiltonian, $\mathcal{H}(\theta)$ with $\theta \in [0.005, 0.065]$ for the $X \ ^1\Sigma_g^+$ block [$p = (-1)^N, S_p = (1 - p)/2, S_e = 0$] and for the $b \ ^3\Sigma_u^+$ block [$p = (-1)^N, S_p = (1 + p)/2, S_e = 1$] with $N = 0, 1$, and 2 total spatial angular momentum quantum numbers. The black triangles indicate the threshold energy of the dissociation continua corresponding to $H(1)+H(1)$, $H(1)+H(2)$, and $H(1)+H(3)$. [Reprinted with permission from E. Mátyus, J. Phys. Chem. A 117, 7195 (2013). Copyright 2013 American Chemical Society.]

TABLE VI: Identified resonance-state energies and widths, in E_h , of H_2 in the $b^3\Sigma_u^+$ block [$p = (-1)^N$, $S_p = (1 + p)/2$, $S_e = 1$] for $N = 0, 1$, and 2.

| (N, p, S_p, S_e) ^a | $\text{Re}(\mathcal{E})$ ^b | $\Gamma/2$ ^b | $E_{\text{Ref,exp}}$ ^c | $E_{\text{Ref,theo}}$ ^d | Assignment ^e |
|---------------------------------|---------------------------------------|-------------------------|-----------------------------------|------------------------------------|-------------------------------|
| $(0, +1, 1, 1)$ | $[-0.999\ 450\ 1]$ ^f | | | $[-0.999\ 455\ 7]$ | H(1)+H(1) continuum |
| | [...] | | | | |
| $(0, +1, 1, 1)$ | $-0.677\ 947\ 1$ | $1 \cdot 10^{-7}$ | $-0.677\ 946\ 1$ | $-0.677\ 942\ 7$ [19] | $e^3\Sigma_u^+, R = 0, v = 0$ |
| $(0, +1, 1, 1)$ | $-0.668\ 549\ 3$ | $9 \cdot 10^{-7}$ | $-0.668\ 547\ 8$ | $-0.668\ 541\ 0$ [19] | $e^3\Sigma_u^+, R = 0, v = 1$ |
| $(1, -1, 0, 1)$ | $[-0.999\ 445\ 8]$ ^f | | | $[-0.999\ 455\ 7]$ | H(1)+H(1) continuum |
| | [...] | | | | |
| $(1, -1, 0, 1)$ | $-0.731\ 434\ 0$ | $5 \cdot 10^{-7}$ | $-0.731\ 438\ 8$ | $-0.731\ 469\ 1$ [20] | $c^3\Pi_u^+, R = 0, v = 0$ |
| $(1, -1, 0, 1)$ | $-0.720\ 717\ 5$ | $2 \cdot 10^{-7}$ | $-0.720\ 782\ 6$ | | $c^3\Pi_u^+, R = 0, v = 1$ |
| | [...] | | | | |
| $(1, -1, 0, 1)$ | $-0.677\ 705\ 5$ | $2 \cdot 10^{-7}$ | $-0.677\ 704\ 1$ | $-0.677\ 698\ 2$ [19] | $e^3\Sigma_u^+, R = 1, v = 0$ |
| $(1, -1, 0, 1)$ | $-0.668\ 319\ 5$ | $1 \cdot 10^{-6}$ | $-0.668\ 319\ 7$ | $-0.668\ 309\ 8$ [19] | $e^3\Sigma_u^+, R = 1, v = 1$ |
| $(2, +1, 1, 1)$ | $[-0.999\ 439\ 7]$ ^f | | | $[-0.999\ 455\ 7]$ | H(1)+H(1) continuum |
| | [...] | | | | |
| $(2, +1, 1, 1)$ | $-0.730\ 888\ 2$ | $9 \cdot 10^{-7}$ | $-0.730\ 888\ 7$ | | $c^3\Pi_u^+, R = 1, v = 0$ |
| $(2, +1, 1, 1)$ | $-0.720\ 219\ 0$ | $< 2 \cdot 10^{-7}$ | $-0.720\ 258\ 0$ | | $c^3\Pi_u^+, R = 1, v = 1$ |
| | [...] | | | | |
| $(2, +1, 1, 1)$ | $-0.677\ 222\ 9$ | $2 \cdot 10^{-8}$ | $-0.677\ 222\ 2$ | | $e^3\Sigma_u^+, R = 2, v = 0$ |
| $(2, +1, 1, 1)$ | $-0.667\ 863\ 2$ | $7 \cdot 10^{-7}$ | $-0.667\ 865\ 3$ | | $e^3\Sigma_u^+, R = 2, v = 1$ |

^a N : total spatial angular momentum quantum number; p : parity, $p = (-1)^N$; S_p and S_e : total spin quantum numbers for the protons and electrons, respectively.

^b $\text{Re}(\mathcal{E})$ and Γ : calculated resonance energy and width with $\Gamma/2 = -\text{Im}(\mathcal{E})$. The largest basis set contained 15 500 basis functions for each set of quantum numbers. The proton-electron ratio was $m_p/m_e = 1\ 836.152\ 672\ 47$ [16].

^c $E_{\text{Ref,exp}}$ experimental reference value, in E_h , derived as $E_{\text{exp}} = E_0 + T_{\text{exp}}$ with the ground-state energy ($X^1\Sigma_g^+, N = 0, v = 0$) $E_0 = -1.164\ 025\ 030\ E_h$. All T_{exp} values were obtained by correcting the experimental term values of Dieke [21], with $-0.000\ 681\ 7\ E_h = -149.63\ \text{cm}^{-1}$ ($1\ E_h = 219\ 474.631\ 4\ \text{cm}^{-1}$), since all triplet term values were too high as it was also noted, for example, in Ref. [19].

^d $E_{\text{Ref,theo}}$: theoretical reference energy, in E_h [19, 20]. The non-relativistic energy of two ground-state hydrogen atoms is given in square brackets.

^e Born–Oppenheimer electronic- and vibrational-state labels. The (approximate) rotational angular momentum quantum number, R , is also given.

^f The lowest-energy eigenvalue of the real Hamiltonian obtained with the largest parameter set and with the given quantum numbers.

- Also note the automated inclusion of the coupling of the orbital and rotational angular momenta

X. MOLECULAR STRUCTURE IN QUANTUM MECHANICS

Equilibrium geometry (IUPAC, Gold Book, last accessed: August 2017):

“Molecular geometry that corresponds to the true minimum on the respective potential energy surface. While information relating to the equilibrium geometry is provided by calculations within the adiabatic approximation (minimization of the total energy with respect to any independent geometrical parameter), various experiments yield some effective geometries for the molecule which are averaged over molecular vibrations.”

- **What is the definition of molecular structure without the BO approximation?**
- **Idea:** let’s look at the wave function!

A. Probabilistic interpretation of the wave function

Claverie and Diner suggested in 1980 that appropriate marginal probability density functions calculated from the full wave function could be used to identify molecular structural features in the full electron-nuclear wave function [22]. In other words, structural parameters do not have sharp, dispersionless values, but they are characterized by some probability density function.

In what follows, one- and two-particle probability density functions are introduced which will be used for the structural analysis. The probability density of selected particles measured from a “center point” P fixed to the body is

$$\begin{aligned} D_{P,a_1 a_2 \dots a_n}^{(n)}(\mathbf{R}_1, \mathbf{R}_2, \dots, \mathbf{R}_n) \\ = \langle \Psi | \delta(\mathbf{r}_{a_1} - \mathbf{r}_P - \mathbf{R}_1) \delta(\mathbf{r}_{a_2} - \mathbf{r}_P - \mathbf{R}_2) \dots \delta(\mathbf{r}_{a_n} - \mathbf{r}_P - \mathbf{R}_n) | \Psi \rangle \end{aligned} \quad (129)$$

with $\mathbf{R}_i \in \mathbb{R}^3$ and the three-dimensional Dirac delta distribution, $\delta(\mathbf{r})$. The center point P can be the center of mass (denoted by “0”) or another particle. For a single

particle, this density function is

$$D_{P,a}^{(1)}(\mathbf{R}_1) = \langle \Psi | \delta(\mathbf{r}_a - \mathbf{r}_P - \mathbf{R}_1) | \Psi \rangle. \quad (130)$$

For $P = 0$, $D_{0,a}^{(1)}$ is the spatial density of particle a around the center of mass (“0”), while for $P = b$, $D_{b,a}^{(1)}$ measures the probability density of the displacement vector connecting a and b .

Due to the overall space rotation-inversion symmetry, $D_{P,a}^{(1)}(\mathbf{R}_1)$ is “round” for $N = 0$, $p = +1$ and the corresponding radial function is:

$$\rho_{P,a}(R) = D_{P,a}^{(1)}(\mathbf{R}_1) \quad (131)$$

with $\mathbf{R}_1 = (0, 0, R)$ and $R \in \mathbb{R}_0^+$. We normalize the density functions to one (so, they measure the fraction of particles which can be found in an infinitesimally small interval dR around R):

$$4\pi \int_0^\infty dR R^2 \rho_{P,a}(R) = 1. \quad (132)$$

The probability density function for the included angle a - P - b is obtained by integrating out the radii in the two-particle density measured from a center point P

$$\Gamma_{P,ab}(\alpha) = \int_0^\infty dR_1 R_1^2 \int_0^\infty dR_2 R_2^2 D_{P,ab}^{(2)}(\mathbf{R}_1, \mathbf{R}_2), \quad (133)$$

with

$$D_{P,ab}^{(2)}(\mathbf{R}_1, \mathbf{R}_2) = \langle \Psi | \delta(\mathbf{r}_a - \mathbf{r}_P - \mathbf{R}_1) \delta(\mathbf{r}_b - \mathbf{r}_P - \mathbf{R}_2) | \Psi \rangle. \quad (134)$$

The center point, P , can be the center of mass ($P = 0$) or another particle ($P = c$). Similarly to $D_{P,a}^{(1)}(\mathbf{R}_1)$, $D_{P,ab}^{(2)}(\mathbf{R}_1, \mathbf{R}_2)$ is also spherically symmetric for wave functions with $N = 0$, $p = +1$, and its numerical value depends only on the lengths $R_1 = |\mathbf{R}_1|$, $R_2 = |\mathbf{R}_2|$, and the α included angle of the vectors \mathbf{R}_1 and \mathbf{R}_2 (for non-zero lengths).

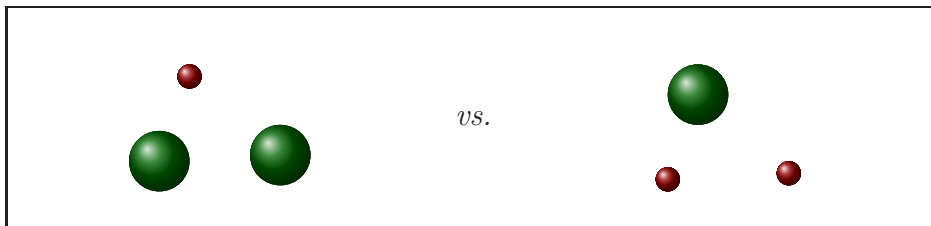


FIG. 9: *In the Born–Oppenheimer approximation “[w]e discuss the very same type of differential equation in an entirely different way”—Hans Primas, Ref. [23].*

We normalize the angle density according to

$$8\pi^2 \int_0^\pi d\alpha \sin \alpha \Gamma_{P,ab}(\alpha) = 1. \quad (135)$$

1. *Numerical demonstration of the $H^- \rightarrow H_2^+$ transition*

In this section, we study the family of $\{a^\pm, a^\pm, b^\mp\}$ -type three-particle Coulomb interacting systems with two identical particles and a third one (Figure 9). This family of systems is described by the Hamiltonian

$$\hat{H}(m_a, m_b, \mathbf{r}) = -\frac{1}{2m_a} \Delta_{\mathbf{r}_1} - \frac{1}{2m_a} \Delta_{\mathbf{r}_2} - \frac{1}{2m_b} \Delta_{\mathbf{r}_3} + \frac{1}{|\mathbf{r}_1 - \mathbf{r}_2|} - \frac{1}{|\mathbf{r}_1 - \mathbf{r}_3|} - \frac{1}{|\mathbf{r}_2 - \mathbf{r}_3|}, \quad (136)$$

for various masses and unit charges. Note that the Hamiltonian is invariant to the inversion of the electric charges. Furthermore, rescaling the masses by a factor η is equivalent to scaling the energy and shrinking the length by the factor η

$$\hat{H}(\eta m_a, \eta m_b, \mathbf{r}) = \eta \hat{H}(m_a, m_b, \eta \mathbf{r}), \quad \forall \eta \in \mathbb{R} \setminus \{0\}. \quad (137)$$

Thereby, it is sufficient to consider only the m_a/m_b mass ratio to obtain qualitatively different solutions. It is also known that the Hamiltonian in Eq. (136) has at least one bound state for all mass ratios.

To numerically study the $H^- \rightarrow H_2^+$ transition, the ground-state wave functions were computed for several mass ratio values using the variational procedure described earlier. Figure 10 shows the transition of the particle density, $D_{0a}^{(1)}$, upon the change of m_a/m_b . It is interesting to note that the emergence of the particle shell is solely

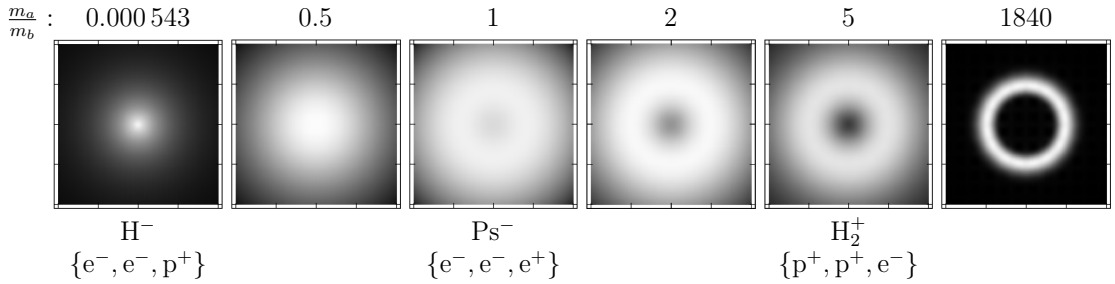


FIG. 10: Transition of the ground-state particle density, $D_{0a}^{(1)}$, by increasing the m_a/m_b mass ratio in $\{a^\pm, a^\pm, b^\mp\}$ -type systems [24]. The center (0) of each plot is the center of mass.

induced by the increase of m_a/m_b [24, 25], while the symmetry-properties of the systems remain unchanged. All systems are “round” in their ground state with $N = 0$ and $p = +1$. In Ref. [24] the transition point was numerically estimated to be between 0.4 and 0.8, which also suggests that the positronium anion, Ps^- , is slightly molecule-like. In the figure the H_2^+ molecular ion is seen as a shell, and thus, we may wonder whether it is possible to identify the relative position of the protons within the shell. For this purpose the angular density function, $\Gamma_{0,pp'}$, was calculated in Ref. [25], which demonstrated that the protons are found at around the antipodal points of the shell (remember that the center of each plot is the center of mass). Kinsey and Fröman [26] and later Woolley [27] have anticipated similar results by considering the “mass polarization” term in the translationally invariant Hamiltonian arising due to the separation of the center of mass. Furthermore, the proton shell has some finite width, which can be interpreted as the zero-point vibration in the BO picture. Recent work [28–30] has elaborated more on the transition properties and vibrational dynamics of this family of three-particle systems and determined the mass ratio where the transition takes place more accurately.

2. Numerical example for a triangular molecule

Larger molecules are also “round” in their eigenstates with zero total angular momentum and positive parity ($N = 0, p = +1$), and localized particles form shells around the molecular center of mass. In order to demonstrate a non-trivial arrangement of the atomic nuclei in a molecule, the $\text{H}_2\text{D}^+ = \{p^+, p^+, d^+, e^-, e^-\}$ molecular ion was studied in Ref. [25]. Interestingly, the qualitative features of the computed

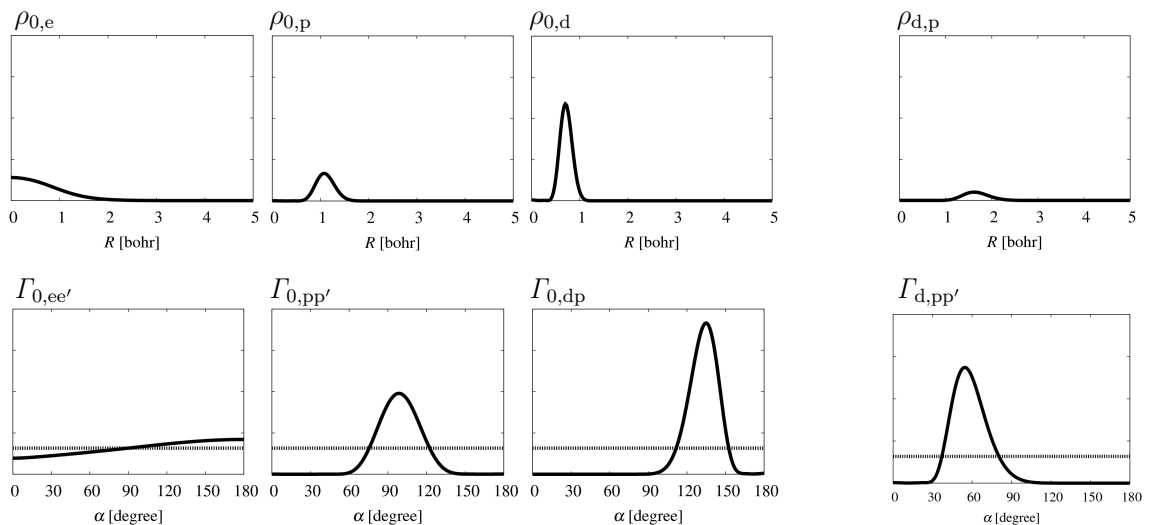


FIG. 11: Probability density functions computed for $\text{H}_2\text{D}^+ = \{e^-, e^-, p^+, p^+, d^+\}$.

density functions (see Figure 11) converged very fast, small basis sets and a loose parameterization was sufficient to observe converged structural features, whereas the energies were far from spectroscopic accuracy.

Figure 11 summarizes the particle-density functions which highlight characteristic structural features of the system. First, we can observe the delocalized electron cloud ($\rho_{0,e}$), the proton shell ($\rho_{0,p}$), and the deuteron shell ($\rho_{0,d}$) around the center of mass. The deuteron shell is more peaked and more localized in comparison with the proton shell. (Remember that these plots show the spherically symmetric density along a ray and all density functions are normalized to one.)

Next, let's look at the probability density functions for the included angle, $\Gamma_{0,ab}$, of two particles measured from the molecular center of mass ("0"). The dashed line in the plots shows the angular density corresponding to a hypothetical system in which the two particles (a and b) are independent. It is interesting to note that for the two electrons $\Gamma_{0,ee'}$ shows very small deviation from the (uncorrelated system's) dashed line. At the same time, we see a pronounced deviation from the dashed line for the nuclei, $\Gamma_{0,pp'}$ and $\Gamma_{0,pd}$. These numerical observations are in line with Claverie and Diner's suggestion based on theoretical considerations [22] that molecular structure could be seen in an fully quantum-mechanical description as correlation effects for the nuclei.

As to the included angle of the two protons and the deuteron, the $\Gamma_{d,pp}$ probability density function has a maximum at around 60 degrees, which indicates the triangular arrangement of the nuclei. Due to the almost negligible amplitude of $\Gamma_{d,pp}$ at around 180 degrees the linear arrangement of the three nuclei (in the ground state) can be excluded. Thus, the pre-BO numerical study is with the molecular (equilibrium) structure known from BO electronic-structure computations.

B. Classical structure from quantum mechanics

Relying on the probabilistic interpretation of quantum mechanics the structure of H_2^+ was visualized as a proton shell (Figure 10) with the protons found at around the antipodal points, and H_2D^+ as a proton shell and a deuteron shell within which the relative arrangement of the three nuclei is dominated by a triangle (Figure 11). This analysis has demonstrated that *elements* of molecular structure can be *recognized* in the appropriate marginal probability densities calculated from the full electron-nuclear wave function. At the same time, a chemist would rather think about H_2^+ as a (classical) rotating dumbbell (Figure 12) and H_2D^+ as a (nearly) equilateral triangle. Although *elements* can be recognized in the probability density functions, the link to the classical structure which chemists have used for more than a century to understand and design new reaction pathways for new materials, is not obvious [23, 27, 31–34]. In order to recover the the classical molecular structure from a fully quantum mechanical treatment, it is necessary to obtain for a molecule

- (a) the shape;
- (b) the handedness: chiral molecules are found exclusively in their left- or right-handed version or a classical mixture (called racemic mixture) of these mirror images but “never” in their superposition;
- (c) the individual labelling of the atomic nuclei (distinguishability).

Although it is possible to write down appropriate linear combinations (wave packets) of eigenstates of the full Hamiltonian, which satisfy these requirements at certain moments, the (a)–(c) properties are well-defined “molecular constants”.

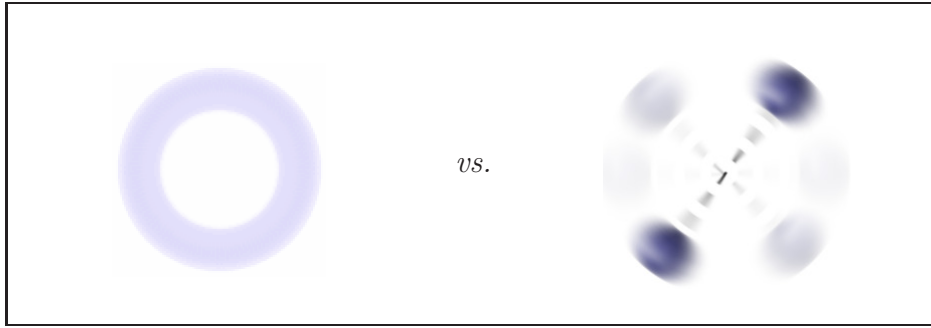


FIG. 12: Superposition vs. a rotating dumbbell

A very successful direction for the resolution of this puzzle is the description of the molecule as an open quantum system being in interaction with an environment [35, 36]. According to decoherence theory pointer states are selected by the continuous monitoring of the environment. As a result, the system's reduced density matrix (after tracing out the environmental degrees of freedom from the world's density matrix) written in this pointer basis evolves in time so that its off-diagonal elements decay exponentially with some decoherence time characteristic to the underlying microscopic interaction process with the environment (radiation or matter). This decay of the off-diagonal elements leads to the suppression of the interference terms between different pointer states, and results in a (reduced) density matrix the form of which corresponds to that of mixed states. Hence, this result can be *interpreted* as the emergence of the classical features in a quantum mechanical treatment. All in all, decoherence theory allows us to identify pointer states, which are selected and remain stable as a result of the molecule's interaction with its environment.

It is interesting to note that important molecular properties (shape, handedness, atomic labels) break the fundamental symmetries of an isolated quantum system: the rotational and inversion symmetry, as well as the indistinguishability of identical particles. It remains a task to explore on a detailed microscopic level how and why these broken-symmetry states become pointer states of a molecular system.

a. Shape Following the pioneering studies which have identified pointer states and confirmed their stability upon translational localization [37–39] Ref. [40] provides a detailed account of the rotational decoherence of mesoscopic objects induced by a photon-gas environment or massive particles in thermal equilibrium. The qualitative conclusions are similar for the two different environments, however there are

differences in the estimated decoherence time and its temperature dependence differ for the two environments. Orientational localization of the mesoscopic ellipsoid takes place only if there are at least two directions for which the electric polarizabilities are different, and coherence is suppressed exponentially with the angular distance between two orientations.

b. Handedness As to the chirality of molecules, the superselection phenomenon has been demonstrated in Ref. [41] by using a master equation [42] which describes the incoherent dynamics of the molecular state in the presence of the scattering of a lighter, thermalized background gas. Experimental conditions are predicted under which the tunneling dynamics is suppressed between the left and right-handed configurations of D_2S_2 .

c. Individual labelling of the atomic nuclei Concerning the distinguishability of atomic nuclei, it remains a challenge to work out the detailed theoretical equations and to estimate the experimental conditions under which the individual labelling of quantum mechanically identical atomic nuclei (*e.g.*, protons) emerges, and gives rise to the concept of chemical isomerism.

Appendix

pdg.lbl.gov/2002/clebrpp.pdf (last accessed: 28 August 2017)

35. CLEBSCH-GORDAN COEFFICIENTS, SPHERICAL HARMONICS, AND d FUNCTIONS

Note: A square-root sign is to be understood over every coefficient, e.g., for $-8/15$ read $-\sqrt{8/15}$. Notation: $\begin{matrix} J & J & \dots \\ M & M & \dots \end{matrix}$

$1/2 \times 1/2$ $\begin{matrix} 1 & & & & \\ +1/2 & +1/2 & & & \\ & & 1 & & \\ & & & 0 & \\ & & & & 0 \end{matrix}$ $Y_1^0 = \sqrt{\frac{3}{4\pi}} \cos \theta$ $2 \times 1/2$ $\begin{matrix} 5/2 & & & & \\ +5/2 & & & & \\ & 5/2 & & 3/2 & \\ +2 & +1/2 & & & \\ & & 1/5 & 4/5 & 5/2 & 3/2 \\ & & 4/5 & -1/5 & +1/2 & +1/2 \end{matrix}$ $\begin{matrix} m_1 & m_2 & & & \\ & & & & \\ m_1 & m_2 & & & \\ & & & & \\ & & & & \\ & & & & \end{matrix}$ Coefficients

$1 \times 1/2$ $\begin{matrix} 3/2 & & & & \\ +3/2 & & & & \\ & 3/2 & & 1/2 & \\ +1 & +1/2 & & & \\ & & 1/3 & 2/3 & 3/2 & 1/2 \\ & & 2/3 & -1/3 & -1/2 & -1/2 \end{matrix}$ $Y_2^0 = \sqrt{\frac{5}{4\pi}} \left(\frac{3}{2} \cos^2 \theta - \frac{1}{2} \right)$ $3/2 \times 1/2$ $\begin{matrix} 7/2 & & & & & & \\ +7/2 & & & & & & \\ & 5/2 & & 3/2 & & & \\ +3/2 & +1/2 & & & & & \\ & & 2/5 & 3/5 & 5/2 & 3/2 \\ & & 3/5 & -2/5 & -1/2 & -1/2 \end{matrix}$

2×1 $\begin{matrix} 3 & & & & & & \\ +3 & & & & & & \\ & 3 & & 2 & & & \\ +2 & +1 & & & & & \\ & & 1/3 & 2/3 & 3/2 & 1/2 \\ & & 2/3 & -1/3 & -1/2 & -1/2 \end{matrix}$ $Y_2^1 = -\sqrt{\frac{15}{8\pi}} \sin \theta \cos \theta e^{i\phi}$ $3/2 \times 1$ $\begin{matrix} 5/2 & & & & & & \\ +5/2 & & & & & & \\ & 5/2 & & 3/2 & & & \\ +3/2 & +1 & & & & & \\ & & 2/5 & 3/5 & 5/2 & 3/2 & 1/2 \\ & & 3/5 & -2/5 & +1/2 & +1/2 & +1/2 \end{matrix}$

1×1 $\begin{matrix} 2 & & & & & & \\ +2 & & & & & & \\ & 2 & & 1 & & & \\ +1 & +1 & & & & & \\ & & 1/5 & 1/3 & 3/5 & & \\ & & 2/5 & -1/2 & 1/10 & & \end{matrix}$ $Y_2^2 = \frac{1}{4} \sqrt{\frac{15}{2\pi}} \sin^2 \theta e^{2i\phi}$ $3/2 \times 1/2$ $\begin{matrix} 7/2 & & & & & & \\ +7/2 & & & & & & \\ & 5/2 & & 3/2 & & & \\ +3/2 & +1/2 & & & & & \\ & & 1/10 & 2/5 & 1/2 & & \\ & & 3/10 & -8/15 & 1/6 & -1/2 & -1/2 & -1/2 \end{matrix}$

$Y_\ell^{-m} = (-1)^m Y_\ell^{m*}$ $d_{m,0}^\ell = \sqrt{\frac{4\pi}{2\ell+1}} Y_\ell^m e^{-im\phi}$ $\begin{matrix} (j_1 j_2 m_1 m_2 | j_1 j_2 J M) \\ = (-1)^{J-j_1-j_2} (j_2 j_1 m_2 m_1 | j_2 j_1 J M) \end{matrix}$

$d_{m',m}^j = (-1)^{m-m'} d_{m,-m'}^j = d_{-m,-m'}^j$ $3/2 \times 3/2$ $\begin{matrix} 7/2 & & & & & & \\ +7/2 & & & & & & \\ & 5/2 & & 3/2 & & & \\ +3/2 & +3/2 & & & & & \\ & & 3/7 & 4/7 & 7/2 & 5/2 & 3/2 \\ & & 4/7 & -3/7 & +3/2 & +3/2 & +3/2 \end{matrix}$ $d_{0,0}^1 = \cos \theta$ $d_{1/2,1/2}^1 = \cos \frac{\theta}{2}$ $d_{1,1}^1 = \frac{1 + \cos \theta}{2}$

2×2 $\begin{matrix} 4 & & & & & & \\ +4 & & & & & & \\ & 4 & & 3 & & & \\ +2 & +2 & & & & & \\ & & 1/2 & 1/2 & 2 & 1 & 0 \\ & & 1/2 & -1/2 & 2 & +2 & +2 \end{matrix}$ $d_{1/2,-1/2}^1 = -\sin \frac{\theta}{2}$ $d_{1,0}^1 = -\frac{\sin \theta}{\sqrt{2}}$ $d_{1,-1}^1 = \frac{1 - \cos \theta}{2}$

$d_{3/2,3/2}^{3/2} = \frac{1 + \cos \theta}{2} \cos \frac{\theta}{2}$ $d_{3/2,1/2}^{3/2} = -\sqrt{3} \frac{1 + \cos \theta}{2} \sin \frac{\theta}{2}$ $d_{3/2,-1/2}^{3/2} = \sqrt{3} \frac{1 - \cos \theta}{2} \cos \frac{\theta}{2}$ $d_{3/2,-3/2}^{3/2} = -\frac{1 - \cos \theta}{2} \sin \frac{\theta}{2}$ $d_{1/2,1/2}^{3/2} = \frac{3 \cos \theta - 1}{2} \cos \frac{\theta}{2}$ $d_{1/2,-1/2}^{3/2} = -\frac{3 \cos \theta + 1}{2} \sin \frac{\theta}{2}$ $d_{2,2}^2 = \left(\frac{1 + \cos \theta}{2} \right)^2$ $d_{2,1}^2 = -\frac{1 + \cos \theta}{2} \sin \theta$ $d_{2,0}^2 = \frac{\sqrt{6}}{4} \sin^2 \theta$ $d_{2,-1}^2 = -\frac{1 - \cos \theta}{2} \sin \theta$ $d_{2,-2}^2 = \left(\frac{1 - \cos \theta}{2} \right)^2$ $d_{1,1}^2 = \frac{1 + \cos \theta}{2} (2 \cos \theta - 1)$ $d_{1,0}^2 = -\sqrt{\frac{3}{2}} \sin \theta \cos \theta$ $d_{1,-1}^2 = \frac{1 - \cos \theta}{2} (2 \cos \theta + 1)$ $d_{0,0}^2 = \left(\frac{3}{2} \cos^2 \theta - \frac{1}{2} \right)$

Figure 35.1: The sign convention is that of Wigner (*Group Theory*, Academic Press, New York, 1959), also used by Condon and Shortley (*The Theory of Atomic Spectra*, Cambridge Univ. Press, New York, 1953), Rose (*Elementary Theory of Angular Momentum*, Wiley, New York, 1957), and Cohen (*Tables of the Clebsch-Gordan Coefficients*, North American Rockwell Science Center, Thousand Oaks, Calif., 1974). The coefficients here have been calculated using computer programs written independently by Cohen and at LBNL.

-
- [1] E. Anderson, Z. Bai, C. Bischof, S. Blackford, J. Demmel, J. Dongarra, J. Du Croz, A. Greenbaum, S. Hammarling, A. McKenney, et al., *LAPACK Users' Guide* (Society for Industrial and Applied Mathematics, Philadelphia, PA, 1999), 3rd ed., ISBN 0-89871-447-8 (paperback).
- [2] M. J. D. Powell, The NEWUOA software for unconstrained optimization without derivatives (DAMTP 2004/NA05), Report no. NA2004/08, <http://www.damtp.cam.ac.uk/user/na/reports04.html> last accessed on January 18, 2013.
- [3] M. Stanke, D. Kedziera, S. Bubin, and L. Adamowicz, *J. Chem. Phys.* **127**, 134107 (2007).
- [4] M. Puchalski and K. Pachucki, *Phys. Rev. A* **78**, 052511 (2008).
- [5] K. L. Sharkley, S. Bubin, and L. Adamowicz, *J. Phys. Chem.* **134**, 044120 (2011).
- [6] K. L. Sharkley, S. Bubin, and L. Adamowicz, *Phys. Rev. A* **83**, 012506 (2011).
- [7] V. I. Korobov, *Phys. Rev. A* **61**, 064503 (2000).
- [8] T. Li and R. Shakeshaft, *Phys. Rev. A* **71**, 052505 (2005).
- [9] Z. Papp, J. Darai, A. Nishimura, Z. T. Hlousek, C.-Y. Hu, and S. L. Yakovlev, *Phys. Lett. A* **304**, 36 (2002).
- [10] S. Bubin and L. Adamowicz, *Phys. Rev. A* **74**, 052502 (2006).
- [11] Y. Suzuki and J. Usukura, *Nuclear Instruments and Methods in Physics Research B* **221**, 195 (2004).
- [12] Y. Suzuki and J. Usukura, *Nuclear Instruments and Methods in Physics Research B* **171**, 67 (2000).
- [13] K. Pachucki and J. Komasa, *J. Chem. Phys.* **130**, 164113 (2009).
- [14] L. Wolniewicz, T. Orlikowski, and G. Staszewska, *J. Mol. Spectrosc.* **238**, 118 (2006).
- [15] L. Wolniewicz, *Mol. Phys.* **105**, 1497 (2007).
- [16] <http://physics.nist.gov/cuu/Constants> (CODATA 2006).
- [17] G. Herzberg, *Spectra of diatomic molecules* (D. Van Nostrand Company, Inc., Princeton, New Jersey, 1950).
- [18] J. Brown and A. Carrington, *Rotational spectroscopy of diatomic molecules* (Cam-

- bridge University Press, Cambridge, 2003).
- [19] W. Kołos and J. Rychlewski, *J. Mol. Spectrosc.* **143**, 237 (1990).
 - [20] W. Kołos and J. Rychlewski, *J. Mol. Spectrosc.* **66**, 428 (1977).
 - [21] G. H. Dieke, *J. Mol. Spectrosc.* **2**, 494 (1958).
 - [22] P. Claverie and S. Diner, *Isr. J. Chem.* **19**, 54 (1980).
 - [23] H. Primas, *Chemistry, Quantum Mechanics and Reductionism: Perspectives in Theoretical Chemistry* (Springer-Verlag, Berlin, 1981).
 - [24] E. Mátyus, J. Hutter, U. Müller-Herold, and M. Reiher, *Phys. Rev. A* **83**, 052512 (2011).
 - [25] E. Mátyus, J. Hutter, U. Müller-Herold, and M. Reiher, *J. Chem. Phys.* **135**, 204302 (2011).
 - [26] A. Fröman and J. L. Kinsey, *Phys. Rev.* **123**, 2077 (1961).
 - [27] R. G. Woolley, *Adv. Phys.* **25**, 27 (1976).
 - [28] F. L. Andrew W. King and H. Cox, *J. Chem. Phys.* **139**, 224306 (2013).
 - [29] A. W. King, L. C. Rhodes, and H. Cox, *Phys. Rev. A* **93**, 022509 (2016).
 - [30] A. L. Baskerville, A. W. King, and H. Cox, *Phys. Rev. A* **94**, 042512 (2016).
 - [31] F. Hund, *Z. Phys.* **43**, 805 (1927).
 - [32] P. Cassam-Chenaï, *J. Math. Chem.* **23**, 61 (1998).
 - [33] B. T. Sutcliffe and R. G. Woolley, *Phys. Chem. Chem. Phys.* **7**, 3664 (2005).
 - [34] B. T. Sutcliffe and R. G. Woolley, *Chem. Phys. Lett.* **408**, 445 (2005).
 - [35] E. Joos, H. Zeh, C. Kiefer, D. Giulini, J. Kupsch, and I. Stamatescu, eds., *Decoherence and the Appearance of a Classical World in Quantum Theory, 2nd edition* (Springer, 2003).
 - [36] M. Schlosshauer, *Decoherence and the Quantum-to-Classical Transition* (Springer, Berlin, 2007).
 - [37] K. Hornberger and J. E. Sipe, *Phys. Rev. A* **68**, 012105 (2003).
 - [38] S. L. Adler, **39**, 14067 (2006).
 - [39] M. Busse and K. Hornberger, **43**, 015303 (2009).
 - [40] C. Zhong and F. Robicheaux, *Phys. Rev. A* **94**, 052109 (2016).
 - [41] J. Trost and K. Hornberger, *Phys. Rev. Lett.* **103**, 023202 (2009).
 - [42] K. Hornberger, *Eur. Phys. Lett.* **77**, 50007 (2007).